

Neutralino Dark Matter in Mirage Mediation

Kiwoon Choi, Kang Young Lee, Yasuhiro Shimizu

Department of Physics, KAIST, Daejeon 305-701, Korea

*E-mail: kchoi@muon.kaist.ac.kr, kylee@muon.kaist.ac.kr,
shimizu@muon.kaist.ac.kr*

Yeong Gyun Kim

*Astrophysical Research Center for the Structure and Evolution of the Cosmos,
Sejong University, Seoul 143-747, Korea*

E-mail: ygkim@muon.kaist.ac.kr

Ken-ichi Okumura

Department of Physics, Kyushu University, Fukuoka 812-8581, Japan

E-mail: okumura@higgs.phys.kyushu-u.ac.jp

ABSTRACT: We study the phenomenology of neutralino dark matter (DM) in mirage mediation scenario of supersymmetry breaking which results from the moduli stabilization in some string/brane models. Depending upon the model parameters, especially the anomaly to modulus mediation ratio determined by the moduli stabilization mechanism, the nature of the lightest supersymmetric particle (LSP) changes from Bino-like neutralino to Higgsino-like one via Bino-Higgsino mixing region. For the Bino-like LSP, the standard thermal production mechanism can give a right amount of relic DM density through the stop/stau-neutralino coannihilation or the pseudo-scalar Higgs resonance process. We also examine the prospect of direct and indirect DM detection in various parameter regions of mirage mediation. Neutralino DM in galactic halo might be detected by near future direct detection experiments in the case of Bino-Higgsino mixed LSP. The gamma ray flux from Galactic Center might be detectable also if the DM density profile takes a cuspy shape.

KEYWORDS: supersymmetry, neutralino dark matter, mirage mediation.

Contents

1.	Introduction	1
2.	Mirage mediation	4
3.	Neutralino DM in intermediate scale mirage mediation	12
3.1	Parameter region of neutralino LSP and thermal relic density	12
3.2	Dark matter detections	16
4.	Neutralino DM for generic mirage messenger scale	19
4.1	Parameter region of neutralino LSP and thermal relic Density	20
4.2	Dark matter detections	25
5.	Conclusions	29

1. Introduction

Low energy supersymmetry (SUSY) is a promising candidate for physics beyond the standard model at TeV scale [1]. In addition to solving the naturalness problem associated with the weak to Planck scale hierarchy $M_{\text{weak}}/M_{Pl} \sim 10^{-16}$, low energy SUSY provide a natural candidate for the cold dark matter (DM) in the universe [2], the neutralino being the lightest supersymmetric particle (LSP), under the assumption of R -parity conservation. The assumption that the LSP neutralino constitutes DM constrains SUSY model in various ways. The first constraint comes from the requirement that the LSP of the model should be a neutralino. Although not severe, the current limits on the direct or indirect detection of DM also provide an additional constraint on the model. Finally, if the mechanism of cosmological neutralino production is specified, the model parameters should be in the range giving the correct DM abundance measured by WMAP [3]:

$$0.085 < \Omega_{DM} h^2 < 0.119. \tag{1.1}$$

Recent development in string moduli stabilization [4, 5] has led to a new pattern of soft SUSY breaking terms which has not been explored before [6]. In KKLT-type moduli stabilization scenario [5], the volume modulus T is stabilized at SUSY AdS vacuum by non-perturbative effect, and this SUSY AdS vacuum of T is lifted to a phenomenologically viable dS or Minkowski vacuum by SUSY breaking brane. Such set-up leads to a mass pattern [6]:

$$\frac{F^T}{T} \sim \frac{m_{3/2}^2}{m_T} \sim \frac{m_{3/2}}{\ln(M_{Pl}/m_{3/2})}, \tag{1.2}$$

where m_T and F^T denote the modulus mass and F -component, respectively. If the SUSY breaking brane is sequestered from the visible sector, the soft masses of visible fields are determined by the modulus mediation [7] of $\mathcal{O}(F^T/T)$ and the anomaly mediation [8] of $\mathcal{O}(m_{3/2}/8\pi^2)$ which are comparable to each other if the gravitino mass $m_{3/2} \sim 10$ TeV as required to give the weak scale size of soft masses. An interesting consequence of this mixed mediation is that soft masses are unified at a mirage messenger scale [9]

$$M_{\text{mir}} = M_{GUT} \left(\frac{m_{3/2}}{M_{Pl}} \right)^{\alpha/2}, \quad (1.3)$$

where α is a parameter of order unity which represents the anomaly to modulus mediation ratio¹. This feature named as mirage mediation [10] is due to the particular property of anomaly mediation which is closely related to the renormalization group (RG) evolution of soft parameters. KKL_T-type moduli stabilization typically gives a positive $\alpha = \mathcal{O}(1)$, and thus a mirage messenger scale hierarchically lower than M_{GUT} . The corresponding low energy superparticle masses have a quite different pattern from those in other SUSY breaking scenarios such as mSUGRA, gauge mediation and anomaly mediation [9, 11, 12, 13].

In this paper, we wish to study some phenomenological aspects of neutralino DM in mirage mediation, particularly examine the parameter range giving LSP neutralino, the relic DM density under the assumption of standard thermal production, and the prospect of direct or indirect detection of DM neutralino. As we will see, when the anomaly to modulus mediation ratio α increases from zero to a positive value of order unity, or equivalently the mirage messenger scale $M_{\text{mir}} = M_{GUT}(m_{3/2}/M_{Pl})^{\alpha/2}$ decreases from M_{GUT} to a hierarchically lower scale, the nature of LSP neutralino is changed from Bino-like to Higgsino-like via Bino-Higgsino mixing region. The enhanced Higgsino component can be understood by the gluino, Wino and Bino mass ratios in mirage mediation:

$$M_3 : M_2 : M_1 \simeq (1 - 0.3\alpha)g_3^2 : (1 + 0.1\alpha)g_2^2 : (1 + 0.66\alpha)g_1^2, \quad (1.4)$$

where $\alpha \neq 0$ represents the effects of anomaly mediation. Thus, compared to the mSUGRA-type pure modulus mediation ($\alpha = 0$), the gluino to Bino mass ratio for $\alpha \sim 1$ is significantly reduced. This results in smaller $|m_{H_u}^2|/M_1^2$ at the weak scale, and thus a smaller Higgsino to Bino mass ratio when the electroweak symmetry breaking condition is imposed. (Here $m_{H_u}^2$ is the soft SUSY breaking mass-square of the up-type Higgs doublet H_u .) As a consequence, for $\alpha \sim 1$, the LSP neutralino has a sizable Higgsino component over a large fraction of the parameter space, and this Higgsino component eventually becomes dominant for a larger value of α . For the parameter region leading to Bino-like LSP, the thermal production mechanism can give a right amount of relic DM density through the stop/stau-neutralino coannihilation process or the pseudo-scalar Higgs resonance effect,

¹Here we are following the notations of Ref. [9]. We warn the readers that some subsequent works [12, 13] are using a differently defined α which corresponds to $\alpha_{\text{Ref.}[12]} = 16\pi^2/[\alpha_{\text{ours}} \ln(M_{Pl}/m_{3/2})] \simeq 4.9/\alpha_{\text{ours}}$. We stress that our definition of α is more convenient for matching the mirage mediation to underlying moduli stabilization model. For instance, the original KKL_T moduli stabilization gives $\alpha_{\text{ours}} = 1$, and many of its generalizations give a rational value of α_{ours} .

depending upon the value of $\tan\beta = \langle H_u \rangle / \langle H_d \rangle$. In overall, compared to mSUGRA scenario, a significantly larger fraction of the parameter space of mirage mediation can give the WMAP DM density under the assumption of the conventional thermal production of neutralino LSP, while satisfying all known phenomenological constraints. As for the DM detection, neutralino DM in galactic halo might be detected by near future direct detection experiments in the case of Bino-Higgsino mixed LSP which can be obtained over a large fraction of the parameter space. The gamma ray flux from galactic center might be detectable also if the DM density profile takes a cuspy shape.

Some phenomenological and cosmological aspects of mirage mediation have been investigated by several groups [9, 11, 12, 13, 14, 15]. In particular, the properties of neutralino DM have been studied in Ref. [13]. The sub-GUT CMSSM model of Ref. [16] also shares a common feature with mirage mediation as it assumes the unification scale of soft parameters below the GUT scale. In this paper, we provide a more extensive analysis of neutralino DM for certain range of model parameters which are expected to be obtained in KKLT-type moduli stabilization scenarios together with a more detailed study of the direct and indirect DM detections. Our results agree qualitatively well with Ref. [13] when the considered parameter space overlaps.

Recent study of moduli cosmology [15] in KKLT-type moduli stabilization indicates that if the early universe underwent a period dominated by the coherent oscillation of moduli, there can be too many gravitinos and neutralino LSPs produced by moduli decays, which would spoil the Big-Bang nucleosynthesis or overclose the universe. This requires a mechanism to dilute the primordial moduli oscillation, e.g. a thermal inflation as proposed in [17]. In the presence of such thermal inflation, the neutralino DM can be produced either by the conventional thermal production mechanism or by the decays of flaton triggering thermal inflation, depending upon the details of reheat procedure. Throughout this paper, we will focus on the relic density of neutralino DM produced by the conventional thermal production mechanism while leaving an additional non-thermal production [15, 18] as an open possibility.

In fact, if the anomaly to modulus mediation ratio α takes a value giving a mirage messenger scale $M_{\text{mir}} = M_{\text{GUT}}(m_{3/2}/M_{\text{Pl}})^{\alpha/2}$ much lower than the intermediate scale, the squark/slepton mass-squares have negative values at certain *high* renormalization point $\mu \gtrsim \mu_c$, although they become positive at lower renormalization point around TeV [9, 12]. As long as the low energy squark/slepton mass-squares are positive², the model has a correct color/charge preserving (but electroweak symmetry breaking) vacuum with squark/slepton fields $\phi = 0$. Still, tachyonic squark/slepton mass-squares at high renormalization point $\mu \gtrsim \mu_c$ might give a deeper color/charge breaking (CCB) minimum or a unbounded from below (UFB) direction in the effective potential at $\phi > \mu_c$ [20], which would make the color/charge conserving vacuum metastable. In the presence of such CCB minimum or UFB direction, there are two points to be clarified to make sure that the model is phenomenologically viable. One first needs a cosmological scenario which allows our universe to be settled down at the correct vacuum, not at the CCB minimum or UFB direction. The second is that the

²It has been argued that a negative stop mass-square at high renormalization point is helpful for ameliorating the fine-tuning for the electroweak symmetry breaking in the MSSM [19].

color/charge preserving vacuum should be stable enough against the tunnelling into CCB minimum or UFB direction. The first point might depend on the detailed history of the early universe. However in view of that squark/sleptons get large positive mass-squares in the high temperature limit, it is a rather plausible assumption that squark/sleptons are settled down at the color/charge preserving minimum after the inflation [21]. As for the vacuum stability, it has been noticed that the potential barrier between $\phi = 0$ and $\phi \gtrsim \mu_c$ gives a tunnelling rate much less than the Hubble expansion rate as long as $\mu_c \gtrsim 10$ TeV [22]. In mirage mediation with positive $\alpha = \mathcal{O}(1)$, once one requires a successful electroweak symmetry breaking, μ_c is higher than 10^3 TeV, thus satisfies safely the stability condition. In this paper, we do not take the existence of CCB minimum or UFB direction at large squark/slepton value $|\phi| \gg 10$ TeV as a serious problem of the model as long as a good color/charge preserving and electroweak symmetry breaking vacuum exists, and focus on the phenomenology of the model under the assumption that we are living in the color/charge preserving local minimum which is stable enough to have a lifetime longer than the age of the universe.

The organization of this paper is as follows. In section II, we review the basic features of mirage mediation. In section III, we examine the prospect of neutralino DM in intermediate scale mirage mediation scenario for several different choices of the matter/Higgs modular weights. In section IV, we extend the analysis to general values of the mirage messenger scale. Section V is the conclusion, and Appendix A contains a summary of our convention and notation.

2. Mirage mediation

Mirage mediation is a natural consequence of the KKLT-type moduli stabilization scenario satisfying the following two assumptions: (i) the modulus T (or dilaton) which determines the standard model gauge couplings is stabilized by non-perturbative effects and (ii) SUSY is broken by a brane-localized source which is sequestered from the visible sector. A well known example of such set-up is the KKLT moduli stabilization [5] in type IIB string theory³ A similar but simpler example would be 5D brane model with a flat interval in one side and an warped interval in other side, in which SUSY breaking brane is introduced at the IR fixed point of the warped interval.

Under these two assumptions, the 4D effective action of the visible sector fields and the gauge coupling modulus T is given by

$$\int d^4\theta \left[-3CC^* e^{-K/3} - C^2 C^{*2} \mathcal{P}_{\text{lift}} \theta^2 \bar{\theta}^2 \right] + \left(\int d^2\theta \left[\frac{1}{4} f_a W^{a\alpha} W_\alpha^a + C^3 W \right] + \text{h.c.} \right), \quad (2.1)$$

where $C = C_0 + F^C \theta^2$ is the chiral compensator superfield, f_a are the holomorphic gauge kinetic function of the visible sector gauge fields, K and W are the effective Kähler potential

³As was noticed in [23, 24], due to the effect of throat vector multiplet, the sequestering might not be precise enough in the case of KKLT compactification of type IIB string theory. The size of non-sequestered soft scalar mass induced by the exchange of throat vector multiplet is quite sensitive to the unknown details of compactification, however there exists a reasonable parameter limit in which the non-sequestered effects can be safely ignored [23].

and superpotential of the visible matter superfields Φ_i and the gauge coupling modulus T , which would be obtained by integrating out heavy moduli. As long as the SUSY breaking brane is sequestered from the visible gauge and matter superfields, its low energy consequence can be described by a simple spurion operator of the form $\mathcal{P}_{\text{lift}}\theta^2\bar{\theta}^2$, independently of the detailed dynamics on the SUSY-breaking brane. Assuming an axionic shift symmetry:

$$U(1)_T : \quad \text{Im}(T) \rightarrow \text{Im}(T) + \text{real constant} \quad (2.2)$$

which is broken by non-perturbative term in the superpotential, the model is given by

$$\begin{aligned} K &= K_0(T + T^*) + Z_i(T + T^*)\Phi_i^*\Phi_i, \\ W &= w - Ae^{-aT} + \frac{1}{6}\lambda_{ijk}\Phi_i\Phi_j\Phi_k, \\ f_a &= kT + \Delta f_a, \\ \mathcal{P}_{\text{lift}} &= \mathcal{P}_{\text{lift}}(T + T^*), \end{aligned} \quad (2.3)$$

where a and k are (discrete) real constants, while $\Delta f_a, w, A$ and λ_{ijk} are complex effective constants obtained after heavy moduli are integrated out. The axionic symmetry (2.2) ensures that K_0, Z_i and $\mathcal{P}_{\text{lift}}$ depend only on $T + T^*$, and a and k are real constant. With these features, the resulting gaugino masses and trilinear A parameters preserve CP as was pointed out in [25].

There might be various ways to generate the modulus superpotential $W_0 = w - Ae^{-aT}$ stabilizing T . Generically the non-perturbative term e^{-aT} can be induced by either a gaugino condensation of T -dependent hidden gauge interaction or a stringy instanton whose Euclidean action is controlled by T . As for the constant term w , it might be induced by a fine-tuned configuration of fluxes as in the original KKLT scenario [5], or alternatively by T -independent non-perturbative effect whose strength is controlled by heavy moduli [26]. As we will see, the non-perturbative stabilization of T by W_0 generates a little hierarchy between the modulus mass and the gravitino mass:

$$\frac{m_T}{m_{3/2}} \sim aT \sim \ln(M_{Pl}/m_{3/2}), \quad (2.4)$$

which results in a little suppression of the modulus F -component:

$$\frac{F^T}{T} \sim \frac{m_{3/2}^2}{m_T} \sim \frac{m_{3/2}}{\ln(M_{Pl}/m_{3/2})}. \quad (2.5)$$

Then, F^T/T naturally has a size comparable to the anomaly mediated soft mass of $\mathcal{O}(m_{3/2}/4\pi^2)$ for the gravitino mass around TeV. If the SUSY breaking source is sequestered from the visible sector, the soft terms of visible fields are determined by the modulus mediation of $\mathcal{O}(F^T/T)$ and the anomaly mediation of $\mathcal{O}(m_{3/2}/4\pi^2)$ which are comparable to each other. This leads to a mirage unification [9] of soft masses at a scale hierarchically different from the gauge coupling unification scale M_{GUT} .

In the Einstein frame, the modulus potential from (2.1) is given by

$$V_{\text{TOT}} = e^{K_0} [(\partial_T\partial_{\bar{T}}K_0)^{-1}|D_TW_0|^2 - 3|W_0|^2] + V_{\text{lift}}, \quad (2.6)$$

where

$$W_0 = w - Ae^{-aT}, \quad V_{\text{lift}} = e^{2K_0/3} \mathcal{P}_{\text{lift}}. \quad (2.7)$$

The superspace lagrangian density (2.1) also determines the auxiliary components of C and T as

$$\begin{aligned} \frac{F^C}{C_0} &= \frac{1}{3} \partial_T K_0 F^T + m_{3/2}^*, \\ F^T &= -e^{K_0/2} (\partial_T \partial_{T^*} K_0)^{-1} (D_T W_0)^*, \end{aligned} \quad (2.8)$$

where $m_{3/2} = e^{K_0/2} W_0$. Note that one can always make both w and A real by appropriate $U(1)_R$ and $U(1)_T$ transformations. In such field basis, the $U(1)_T$ invariance of K_0 assures that both $m_{3/2}$ and F^T are real. In the following, we will use this field basis in which the CP invariance of soft parameters is easier to be recognized.

To stabilize T at a reasonably large value while having $m_{3/2}$ hierarchically smaller than M_{Pl} , one needs to assume that w is hierarchically smaller than A in the unit with $M_{Pl} = 1$. Since $w \sim m_{3/2}$ and one needs $m_{3/2} \sim 10$ TeV to get the weak scale superparticle masses, $\ln(A/w)$ typically has a value of $\mathcal{O}(4\pi^2)$. It is then straightforward to compute the vacuum values of T and F^T by minimizing the modulus potential (2.6) under the fine tuning condition $\langle V_{\text{TOT}} \rangle = 0$. At leading order in $\epsilon = 1/\ln(A/w)$, one finds [6]

$$\begin{aligned} aT &\simeq \ln(A/w), \\ \frac{F^T}{T + T^*} &\simeq \frac{m_{3/2}}{\ln(A/w)} \left(1 + \frac{3\partial_T \ln(\mathcal{P}_{\text{lift}})}{2\partial_T K_0} \right), \end{aligned} \quad (2.9)$$

which shows that F^T/T is indeed of the order of $m_{3/2}/4\pi^2$ for $\ln(A/w) \sim 4\pi^2$.

Let us consider the soft terms of canonically normalized visible fields derived from the 4D effective action (2.1):

$$\mathcal{L}_{\text{soft}} = -\frac{1}{2} M_a \lambda^a \lambda^a - \frac{1}{2} m_i^2 |\phi_i|^2 - \frac{1}{6} A_{ijk} y_{ijk} \phi_i \phi_j \phi_k + \text{h.c.}, \quad (2.10)$$

where λ^a are gauginos, ϕ_i are the scalar component of Φ_i and y_{ijk} are the canonically normalized Yukawa couplings:

$$y_{ijk} = \frac{\lambda_{ijk}}{\sqrt{e^{-K_0} Z_i Z_j Z_k}}. \quad (2.11)$$

For $F^T/T \sim m_{3/2}/4\pi^2$, the soft parameters at energy scale just below M_{GUT} are determined by the modulus-mediated and anomaly-mediated contributions which are comparable to each other. One then finds [6]

$$\begin{aligned} M_a &= M_0 + \frac{m_{3/2}}{16\pi^2} b_a g_a^2, \\ A_{ijk} &= \tilde{A}_{ijk} - \frac{m_{3/2}}{16\pi^2} (\gamma_i + \gamma_j + \gamma_k), \\ m_i^2 &= \tilde{m}_i^2 - \frac{m_{3/2}}{16\pi^2} M_0 \theta_i - \left(\frac{m_{3/2}}{16\pi^2} \right)^2 \dot{\gamma}_i \end{aligned} \quad (2.12)$$

where M_0 , \tilde{A}_{ijk} and \tilde{m}_i are the pure modulus-mediated gaugino mass, trilinear A -parameters and sfermion masses which are given by

$$\begin{aligned}
 M_0 &= F^T \partial_T \ln \text{Re}(f_a), \\
 \tilde{m}_i^2 &= -F^T F^{T*} \partial_T \partial_{\bar{T}} \ln(e^{-K_0/3} Z_i), \\
 \tilde{A}_{ijk} &= -F^T \partial_T \ln \left(\frac{\lambda_{ijk}}{e^{-K_0} Z_i Z_j Z_k} \right) = F^T \partial_T \ln(e^{-K_0} Z_i Z_j Z_k) \\
 &= \tilde{A}_i + \tilde{A}_j + \tilde{A}_k \quad \text{for} \quad \tilde{A}_i = F^T \partial_T \ln(e^{-K_0/3} Z_i).
 \end{aligned} \tag{2.13}$$

Here we have used that the holomorphic Yukawa couplings λ_{ijk} are T -independent constants as a consequence of the axionic shift symmetry $U(1)_T$, and the one-loop beta function coefficient b_a , the anomalous dimension γ_i and its derivative $\dot{\gamma}_i$, and θ_i are defined as

$$\begin{aligned}
 b_a &= -3\text{tr}(T_a^2(\text{Adj})) + \sum_i \text{tr}(T_a^2(\phi_i)), \\
 \gamma_i &= 2 \sum_a g_a^2 C_2^a(\phi_i) - \frac{1}{2} \sum_{jk} |y_{ijk}|^2, \\
 \dot{\gamma}_i &= 8\pi^2 \frac{d\gamma_i}{d \ln \mu}, \\
 \theta_i &= 4 \sum_a g_a^2 C_2^a(\phi_i) - \sum_{jk} |y_{ijk}|^2 \frac{\tilde{A}_{ijk}}{M_0},
 \end{aligned} \tag{2.14}$$

where the quadratic Casimir $C_2^a(\phi_i) = (N^2 - 1)/2N$ for a fundamental representation ϕ_i of the gauge group $SU(N)$, $C_2^a(\phi_i) = q_i^2$ for the $U(1)$ charge q_i of ϕ_i , and $\omega_{ij} = \sum_{kl} y_{ikl} y_{jkl}^*$ is assumed to be diagonal. In Appendix A, we provide a summary of our convention and notation.

For our later discussion, it is convenient to define

$$\alpha \equiv \frac{m_{3/2}}{M_0 \ln(M_{Pl}/m_{3/2})}, \quad a_i \equiv \frac{\tilde{A}_i}{M_0}, \quad c_i \equiv \frac{\tilde{m}_i^2}{M_0^2}, \tag{2.15}$$

where α represents the anomaly to modulus mediation ratio, while a_i and c_i parameterize the pattern of the pure modulus mediated soft masses. Then the boundary values of soft parameters at M_{GUT} are given by

$$\begin{aligned}
 M_a &= M_0 \left[1 + \frac{\ln(M_{Pl}/m_{3/2})}{16\pi^2} b_a g_a^2 \alpha \right], \\
 A_{ijk} &= M_0 \left[(a_i + a_j + a_k) - \frac{\ln(M_{Pl}/m_{3/2})}{16\pi^2} (\gamma_i + \gamma_j + \gamma_k) \alpha \right], \\
 m_i^2 &= M_0^2 \left[c_i - \frac{\ln(M_{Pl}/m_{3/2})}{16\pi^2} \theta_i \alpha - \left(\frac{\ln(M_{Pl}/m_{3/2})}{16\pi^2} \right)^2 \dot{\gamma}_i \alpha^2 \right],
 \end{aligned} \tag{2.16}$$

where

$$\theta_i = 4 \sum_a g_a^2 C_2^a(\phi_i) - \sum_{jk} |y_{ijk}|^2 (a_i + a_j + a_k). \tag{2.17}$$

In this prescription, generic mirage mediation is parameterized by

$$M_0, \alpha, a_i, c_i, \tan \beta, \quad (2.18)$$

where we have replaced the Higgs mass parameters μ and B by $\tan \beta = \langle H_u \rangle / \langle H_d \rangle$ and M_Z as usual. As we will see, this parameterization of mirage mediation is particularly convenient when one compute the mirage mediation parameters from underlying SUGRA model. For instance, α , a_i and c_i are given by simple rational numbers in minimal KKLT-type moduli stabilization.

Taking into account the 1-loop RG evolution, the soft masses of (2.12) at M_{GUT} leads to low energy soft masses which can be described in terms of the mirage messenger scale:

$$M_{\text{mir}} = \frac{M_{GUT}}{(M_{Pl}/m_{3/2})^{\alpha/2}}. \quad (2.19)$$

For instance, the low energy gaugino masses are given by [9]

$$M_a(\mu) = M_0 \left[1 - \frac{1}{8\pi^2} b_a g_a^2(\mu) \ln \left(\frac{M_{\text{mir}}}{\mu} \right) \right] = \frac{g_a^2(\mu)}{g_a^2(M_{\text{mir}})} M_0, \quad (2.20)$$

showing that the gaugino masses are unified at M_{mir} , while the gauge couplings are unified at M_{GUT} . The low energy values of A_{ijk} and m_i^2 generically depend on the associated Yukawa couplings y_{ijk} . However if y_{ijk} are small enough or

$$a_i + a_j + a_k = c_i + c_j + c_k = 1 \quad \text{for} \quad y_{ijk} \sim 1, \quad (2.21)$$

their low energy values are given by [9]

$$\begin{aligned} A_{ijk}(\mu) &= M_0 \left[a_i + a_j + a_k + \frac{1}{8\pi^2} (\gamma_i(\mu) + \gamma_j(\mu) + \gamma_k(\mu)) \ln \left(\frac{M_{\text{mir}}}{\mu} \right) \right], \\ m_i^2(\mu) &= M_0^2 \left[c_i - \frac{1}{8\pi^2} Y_i \left(\sum_j c_j Y_j \right) g_Y^2(\mu) \ln \left(\frac{M_{GUT}}{\mu} \right) \right. \\ &\quad \left. + \frac{1}{4\pi^2} \left\{ \gamma_i(\mu) - \frac{1}{2} \frac{d\gamma_i(\mu)}{d \ln \mu} \ln \left(\frac{M_{\text{mir}}}{\mu} \right) \right\} \ln \left(\frac{M_{\text{mir}}}{\mu} \right) \right], \end{aligned} \quad (2.22)$$

where Y_i is the $U(1)_Y$ charge of ϕ_i . Quite often, the modulus-mediated squark and slepton masses have a common value, i.e. $c_{\tilde{q}} = c_{\tilde{l}}$. Then, according to the above expression of low energy sfermion mass, the 1st and 2nd generation squark and slepton masses are unified again at the mirage messenger scale M_{mir} .

In KKLT compactification of type IIB string theory [5], T corresponds to the Calabi-Yau volume modulus, and the uplifting brane is located at the end of warped throat. In this case, the uplifting operator is sequestered from T [6]:

$$\partial_T \mathcal{P}_{\text{lift}} = 0. \quad (2.23)$$

Also, the minimal KKLT compactification of IIB theory gives

$$\begin{aligned} K_0 &= -3 \ln(T + T^*), \quad Z_i = \frac{1}{(T + T^*)^{n_i}}, \\ f_a &= kT, \quad W_0 = w - A e^{-aT} \quad (A = \mathcal{O}(1)), \end{aligned} \quad (2.24)$$

where the modular weight n_i is a rational number depending on the origin of matter superfield Φ_i . Then from (2.13) and (2.9), one immediately finds

$$\alpha = 1, \quad a_i = c_i = 1 - n_i, \tag{2.25}$$

giving an intermediate mirage messenger scale:

$$M_{\text{mir}} \sim 3 \times 10^9 \text{ GeV}. \tag{2.26}$$

If Φ_i lives on the entire world-volume of $D7$ brane from which the visible gauge bosons originate, the corresponding modular weight $n_i = 0$. However, if Φ_i is confined in the intersections of $D7$ branes, n_i has a positive value, e.g. $n_i = 1/2$ or 1. In Fig. 1, we depict the RG evolution of gauge couplings and soft masses in intermediate scale mirage mediation scenario with $n_i = 0$, i.e. $\alpha = a_i = c_i = 1$, which shows that indeed the gaugino masses and the 1st and 2nd generations of squarks and slepton masses are unified at $M_{\text{mir}} \sim 3 \times 10^9$ GeV as indicated by (2.20) and (2.22). Note that still the gauge couplings are unified at the conventional GUT scale $M_{GUT} \sim 2 \times 10^{16}$ GeV. In view of its minimality, intermediate scale mirage mediation can be considered as a benchmark scenario, thus we perform a detailed analysis of neutralino DM in intermediate scale mirage mediation in the next section.

It is in fact easy to generalize the compactification to get different values of the mirage mediation parameters α , a_i and c_i . For instance, the compactification can be generalized to have a dilaton-modulus mixing in gauge kinetic functions [27, 28] and/or the non-perturbative superpotential [29]. For the case of type IIB compactification, a nonzero gauge flux on $D7$ branes can generate such dilaton-modulus mixing in $D7$ gauge kinetic functions [28], which would result in

$$f_a = kT + lS_0, \quad W_0 = w - Ae^{-(aT+bS_0)} \quad (A = \mathcal{O}(1)), \tag{2.27}$$

where S_0 denotes the vacuum value of the string dilaton S which is assumed to get super-heavy mass from RR and NS-NS 3-form fluxes, and k, l, a and b are real parameters. In such IIB compactifications, the coefficients of T in $D7$ gauge kinetic functions and non-perturbative superpotential, i.e. k and a , are positive, however the coefficients of S , i.e. l and b , might have both signs under the conditions:

$$\begin{aligned} k\text{Re}(T) + l\text{Re}(S_0) &\simeq \frac{1}{g_{GUT}^2} \simeq 2, \\ a\text{Re}(T) + b\text{Re}(S_0) &\simeq \ln(M_{Pl}/m_{3/2}) \simeq 4\pi^2. \end{aligned} \tag{2.28}$$

Assuming that $e^{-K_0/3}Z_i$ has the same form as the minimal model (2.24), it is then straightforward to find that the mirage mediation parameters are given by

$$\begin{aligned} \alpha &= \frac{1 + R_1}{(1 + R_2)(1 + R_3)}, \\ a_i &= (1 - n_i)(1 + R_1), \\ c_i &= (1 - n_i)(1 + R_1)^2 \end{aligned} \tag{2.29}$$

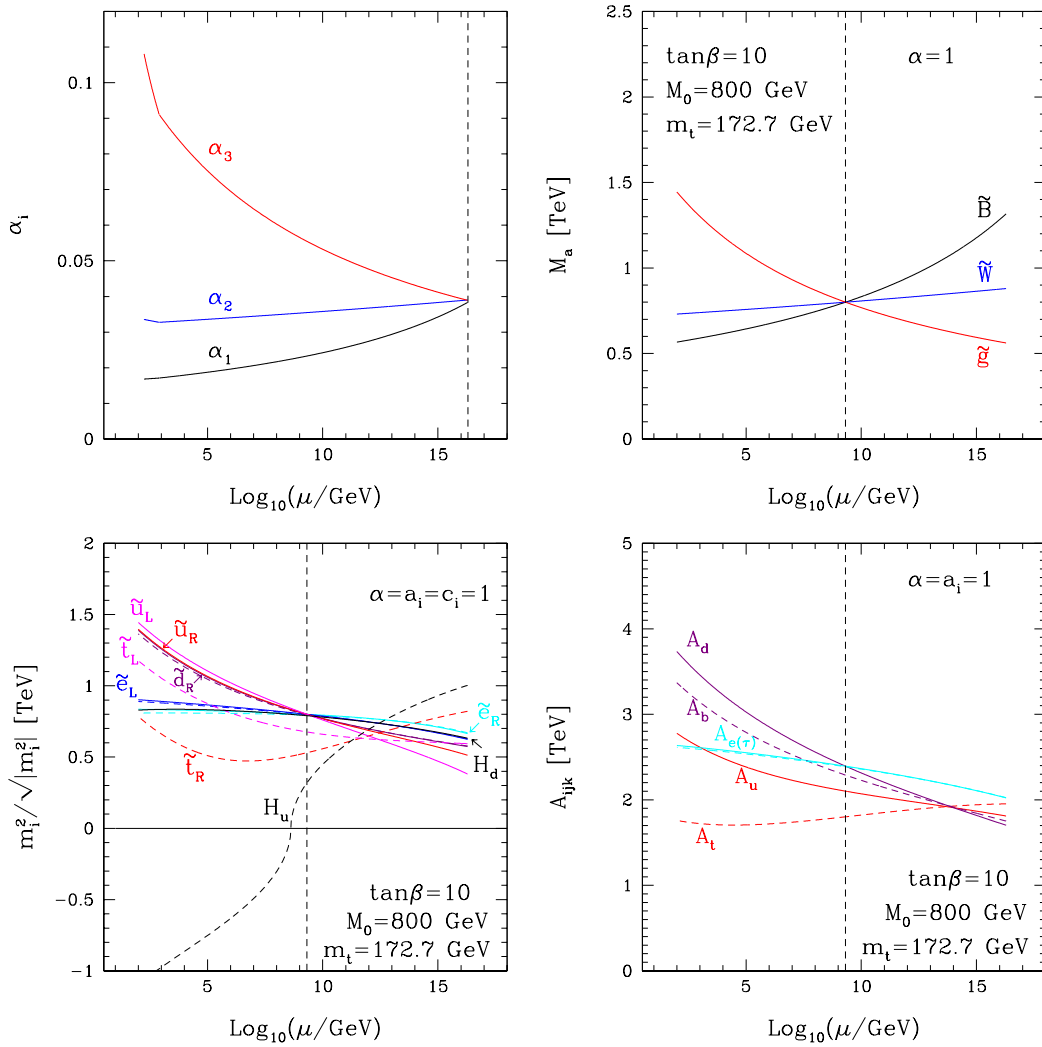


Figure 1: RG evolution of (a) gauge couplings α_i , (b) gaugino masses M_a , (c) sfermion and Higgs masses m_i , (d) trilinear A parameters in intermediate scale mirage mediation with $a_i = c_i = 1$. Here we choose $M_0 = 800$ GeV and $\tan\beta = 10$.

where

$$R_1 = \frac{l\text{Re}(S_0)}{k\text{Re}(T)}, \quad R_2 = \frac{b\text{Re}(S_0)}{a\text{Re}(T)}, \quad R_3 = \frac{3\partial_T \ln(\mathcal{P}_{\text{lift}})}{2\partial_T K_0}. \quad (2.30)$$

Again, for $\mathcal{P}_{\text{lift}}$ induced by an uplifting brane at the end of warped throat, $R_3 = 0$. However, $1 + R_1$ and $1 + R_2$ can have a variety of (positive) values under the condition (2.28). As a result, the anomaly to modulus mediation ratio α can easily have any (positive) value within the range of order unity.

A particularly interesting model is the TeV scale mirage mediation with

$$\alpha = 2, \quad a_{H_u} = c_{H_u} = 0, \quad a_{Q_3} + a_{U_3} = c_{Q_3} + c_{U_3} = 1, \quad (2.31)$$

where Q_3 and U_3 denote the left-handed and right handed top-quark superfields, respectively. This particular model has been claimed to minimize the fine tuning for the elec-

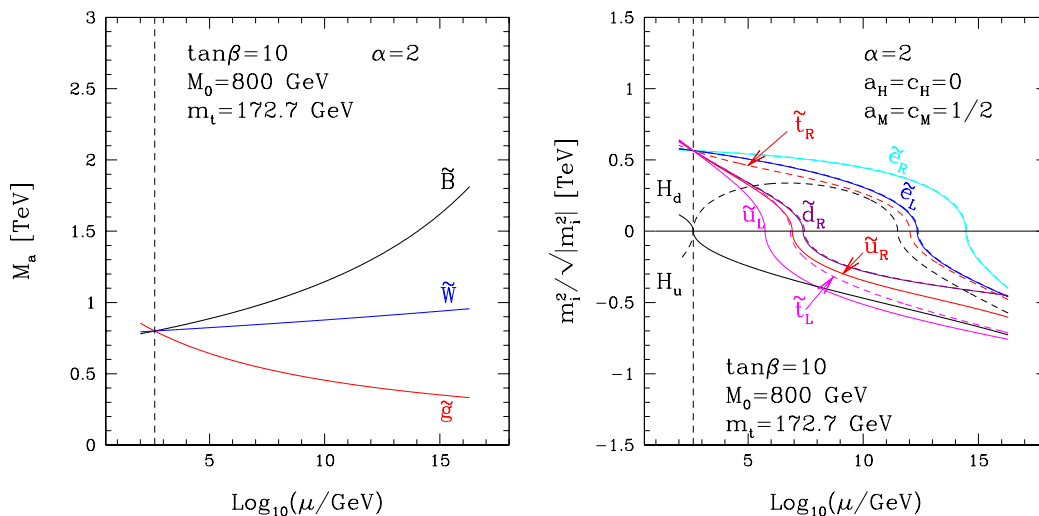


Figure 2: RG evolution of (a) gaugino masses and (b) sfermion and Higgs masses in TeV scale mirage mediation. Here we fixed $M_0 = 800$ GeV, $a_H = c_H = 0$ and $a_M = c_M = 1/2$.

troweak symmetry breaking in the MSSM [30]. In Fig. 2, we depict the RG evolution of soft masses in TeV scale mirage mediation model with $a_H = c_H = 0$ and $a_M = c_M = 1/2$, where the subscripts H and M stands for the MSSM Higgs doublets $H_{u,d}$ and the quark/lepton matter superfields, respectively.

Note that the squark/slepton mass-squares renormalized at high energy scale, e.g. at a scale near M_{GUT} , are negative in this model, while the values at low energy scale below 10^6 GeV are positive. In fact, such tachyonic *high energy* squark/slepton mass-squares is a generic feature of mirage mediation for $\alpha > \alpha_c$ where the precise value of α_c depends on a_i and c_i , but not significantly bigger than 1 in most cases. As long as the low energy squark/slepton mass-squares are positive, the model has a correct color/charge preserving (but electroweak symmetry breaking) vacuum. For instance, the TeV scale mirage mediation model of Fig. 2 has a such vacuum which is a local minimum of the scalar potential over the squark/slepton values $|\phi| \lesssim 10^6$ GeV. On the other hand, tachyonic squark mass-squares at the RG point $\mu > 10^6$ GeV indicates that there might be a deeper CCB minimum color/charge breaking (CCB) or an unbounded from below (UFB) direction at $|\phi| > 10^6$ GeV. One then needs a cosmological scenario which allows our universe to be settled down at the correct vacuum with $\phi = 0$. In view of that the squarks and sleptons get large positive mass-squares in the high temperature limit, it is rather plausible assumption that squark/sleptons are settled down at the color/charge preserving minimum after the inflation [21]. One still needs to confirm that the color/charge preserving vacuum is stable enough against the decay into CCB vacuum. It has been noticed that the corresponding tunnelling rate is small enough, i.e. less than the Hubble expansion rate, as long as the RG points of vanishing squark/slepton mass-squares are all higher than 10^4 GeV [22, 21], which is satisfied safely by the TeV scale mirage mediation of Fig. 2.

3. Neutralino DM in intermediate scale mirage mediation

In this section, we examine the prospect of neutralino DM in intermediate scale mirage mediation scenario. As was noticed in the previous section, the minimal KKLT-type model (2.24) with a sequestered uplifting brane gives $\alpha = 1$, thus an intermediate mirage messenger scale

$$M_{\text{mir}} \sim M_{GUT}(m_{3/2}/M_{Pl})^{1/2} \sim 3 \times 10^9 \text{ GeV}. \quad (3.1)$$

In this minimal set-up, the discrete parameters a_i and c_i describing the modulus mediated A -parameters and sfermion masses are determined to be $a_i = c_i = 1 - n_i$, where n_i denote the modular weights of matter and Higgs superfields. Throughout this paper, we will assume $a_i = c_i$ and consider the following four different cases:

$$(a_H = c_H, a_M = c_M) = (1, 1), \quad \left(\frac{1}{2}, \frac{1}{2}\right), \quad (0, 1), \quad \left(0, \frac{1}{2}\right). \quad (3.2)$$

We also choose the Higgsino mass parameter $\mu > 0$ in light of the experimental value of the muon anomalous magnetic moment which favors positive μ [31], and treat $\tan\beta = \langle H_u \rangle / \langle H_d \rangle$ as a free parameter without specifying the origin of the corresponding μ and B parameters. We then obtain the parameter range of the model for which the LSP is the lightest neutralino as well as the relic neutralino DM abundance under the assumption of thermal production, and finally the direct and indirect detection rates of the neutralino LSP using the DarkSUSY routine [32].

3.1 Parameter region of neutralino LSP and thermal relic density

In Fig. 3, we show the neutralino LSP region and the thermal neutralino relic density in intermediate scale mirage mediation scenario on the $(\tan\beta, M_0)$ -plane for the values of a_i and c_i specified in Eq. (3.2). We computed the sparticle mass spectrum at the electroweak scale by solving the RG equations with the boundary condition (2.12) at M_{GUT} . Our results show that in all cases there is a large parameter region for which the LSP is given by the lightest neutralino.

Fig. 3.a is the result for the case in which $a_i = c_i = 1$ for both matter and Higgs multiplets. In this case, large $\tan\beta > 34$ (grey color) for which the tau Yukawa couplings becomes sizable gives stau LSP (see also Fig. 4.a), while small $M_0 \lesssim 0.5 \text{ TeV}$ (green color) gives stop LSP. In the remaining region, the LSP is the lightest neutralino which turns out to be Bino-like. Small $\tan\beta \lesssim 3$ is excluded by the Higgs mass limit $m_h > 114 \text{ GeV}$. Under the assumption that the DM neutralinos are produced purely by the conventional thermal production mechanism, the magenta stripe corresponds to the parameter region giving a relic neutralino density consistent with the recent WMAP observation [3]:

$$0.085 < \Omega_{\text{DM}} h^2 < 0.119 \quad (2\sigma \text{ level}). \quad (3.3)$$

In the region below the magenta stripe, $\Omega_\chi h^2 < 0.085$, while $\Omega_\chi h^2 > 0.119$ for the upper region. Thus the (cyan) region below the magenta stripe (but above the stop LSP region)

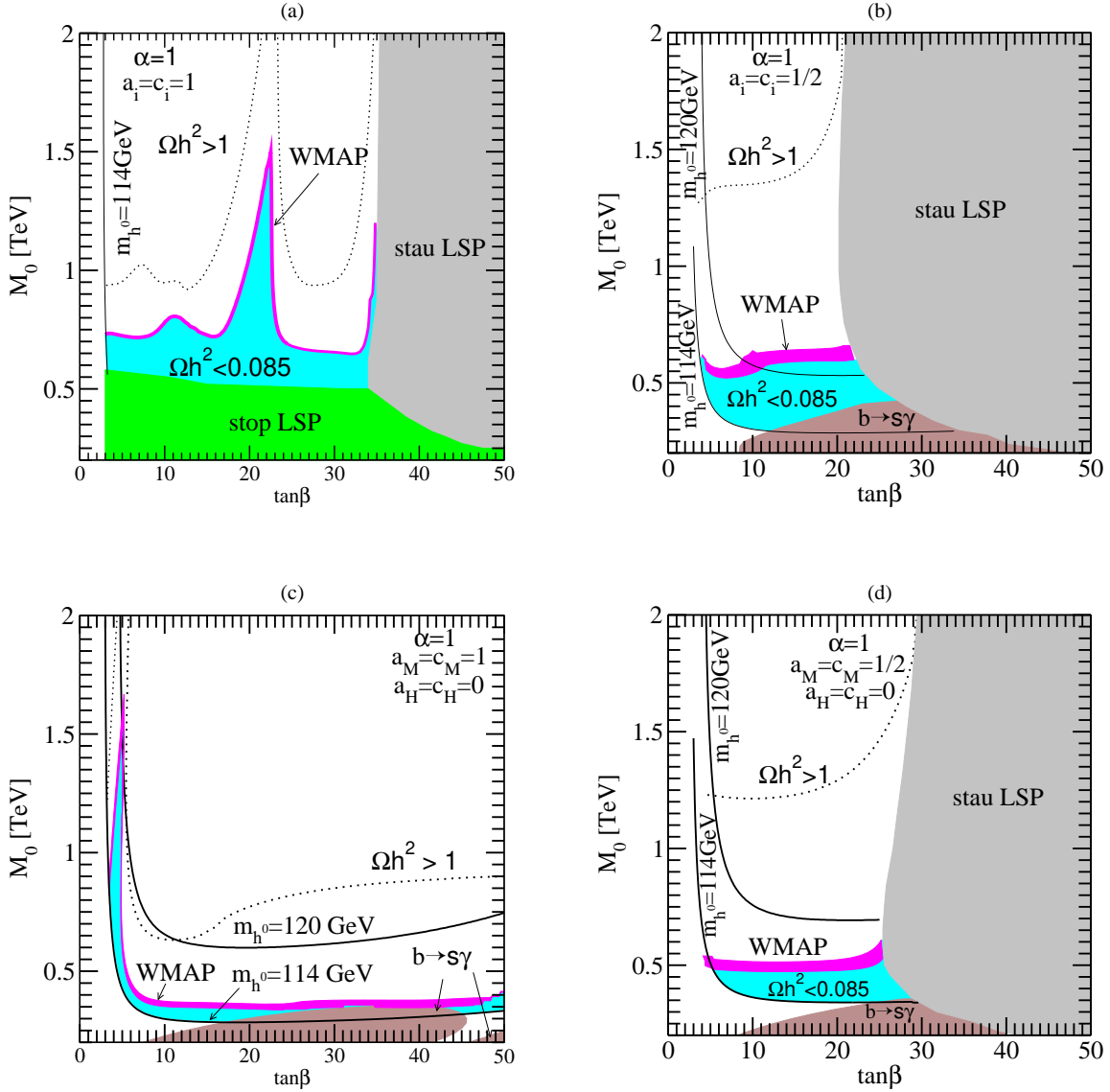


Figure 3: Parameter region of neutralino LSP and the thermal relic density depicted on the plane of $(\tan\beta, M_0)$ in intermediate scale mirage mediation models with (a_i, c_i) specified in Eq. (3.2).

can be phenomenologically viable if additional DM neutralinos were produced by non-thermal mechanism such as the decays of flaton in thermal inflation [17].

Although the neutralino LSP is Bino-like in this particular intermediate scale mirage mediation, the WMAP mass density is obtained for a rather heavy neutralino mass $m_{\chi_0} \gtrsim 450$ GeV. This can be understood by Fig. 4.a which shows the masses of the lightest neutralino, lighter stop and stau, and also the pseudo-scalar Higgs boson as a function of $\tan\beta$ for the model with $\alpha = 1$, $a_i = c_i = 1$ and $M_0 = 800$ GeV. Around $\tan\beta \sim 20$, the pseudoscalar Higgs mass becomes same as $2m_{\chi_0}$, leading to a resonant enhancement of neutralino annihilation through the s-channel pseudo-scalar Higgs exchange. For other values of $\tan\beta$, the neutralino mass is somewhat close to the stop mass (or to the stau

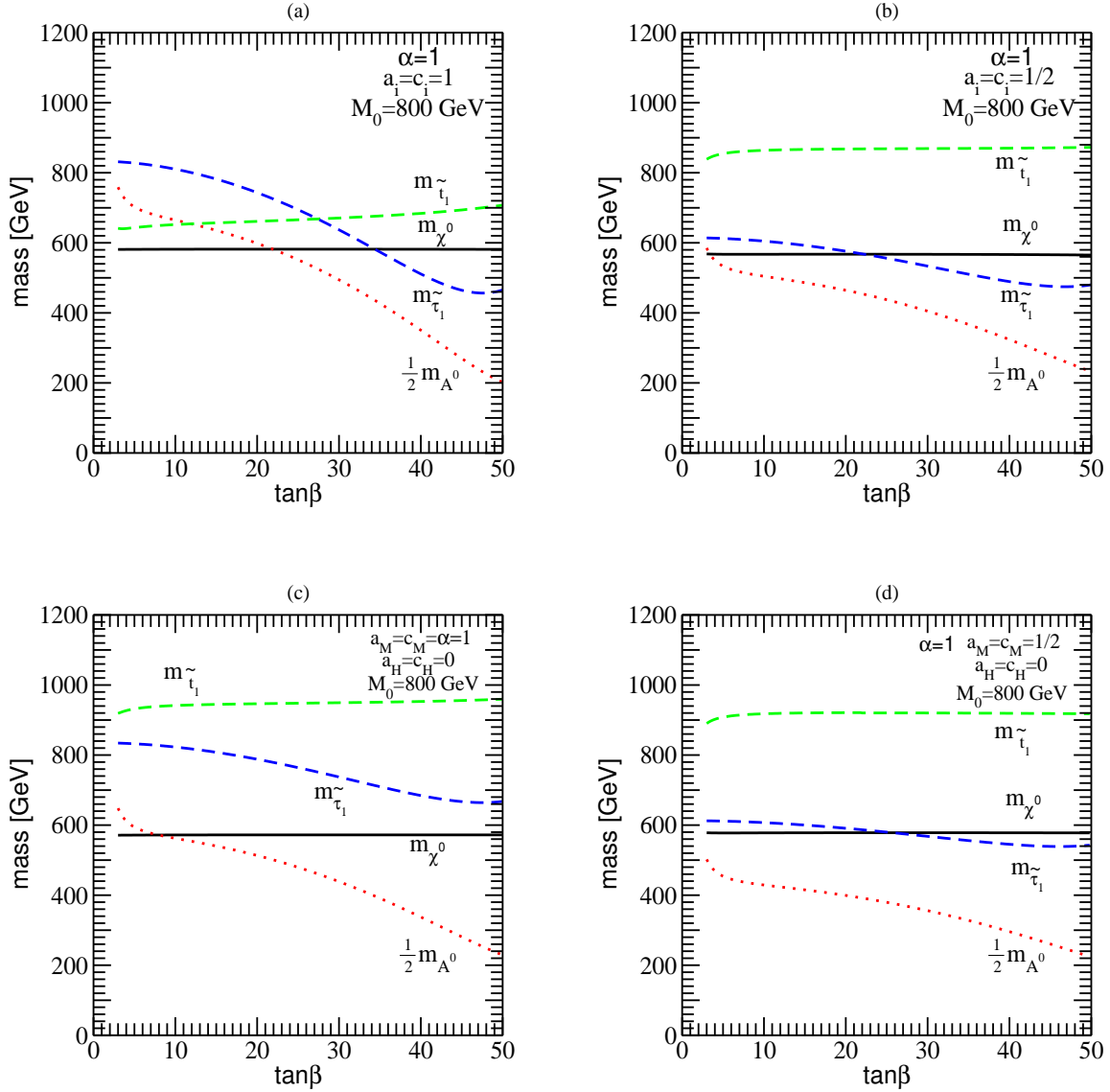


Figure 4: Particle masses as a function of $\tan\beta$ in intermediate scale mirage mediation models with (a_i, c_i) specified in Eq. (3.2). Here, we fixed $M_0 = 800$ GeV.

mass at $\tan\beta \sim 34$), making the stop-neutralino or stau-neutralino coannihilation process becomes efficient. In Fig. 5, we depicted $\Omega_\chi h^2$ as a function of $\tan\beta$ for $M_0 = 800$ GeV, which shows clearly the effect of Higgs resonance at $\tan\beta \sim 20$ and also the effect of stop/stau coannihilation effects for other values of $\tan\beta$. On the plot, the dotted line corresponds to the relic density computed without including coannihilation effects. It indicates that the stop/stau-neutralino coannihilation plays a crucial role for the relic neutralino density to have the WMAP value (3.3) for $M_0 = 700 \sim 800$ GeV and $\tan\beta$ outside the Higgs resonance region. Note that in intermediate scale mirage mediation with $a_i = c_i = 1$, the pseudoscalar Higgs resonance condition $m_A \simeq 2m_\chi$ is satisfied for smaller value of $\tan\beta$ compared to the mSUGRA case. This can be understood by noting that

the low energy gaugino masses in mirage mediation are more compressed compared to mSUGRA, e.g. $M_3/M_1 \sim 2.3$ in the intermediate scale mirage mediation with $\alpha = 1$, while $M_3/M_1 \sim 6$ in mSUGRA. For a given value of M_1 , smaller M_3 gives smaller μ and $m_A^2 \sim m_{H_d}^2 + \mu^2$ at the electroweak scale, thus the pseudoscalar Higgs resonance appears at smaller value of $\tan\beta$ compared to mSUGRA case.

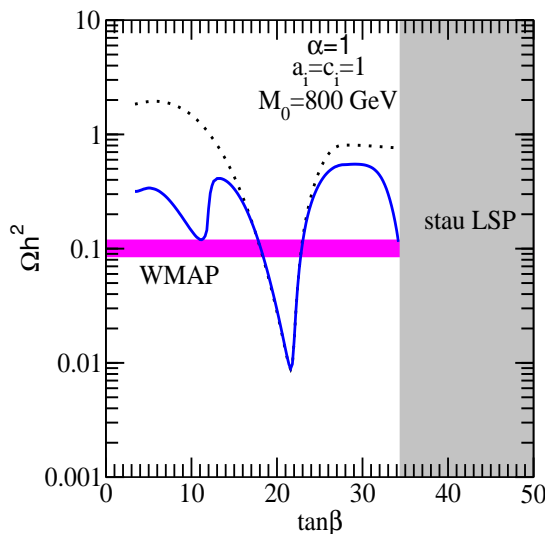


Figure 5: $\Omega_\chi h^2$ as a function of $\tan\beta$ in intermediate scale mirage mediation with $a_i = c_i = 1$ and $M_0 = 800$ GeV. Here the dotted line corresponds to the result computed without including the stop/stau coannihilation effects.

So far, we have been focusing on the specific intermediate scale mirage mediation model with $a_i = c_i = 1$ which might be obtained when all modular weights $n_i = 0$. However as anticipated in the previous section, $a_i = c_i = 1$ is not necessarily a more favored choice than the other values of (a_i, c_i) in Eq. (3.2). Different values of a_i and c_i , e.g. smaller but still non-negative values, are also equally plausible. Obviously, for a fixed value of M_0 , the gaugino masses are not affected by changing a_i and c_i . However the low energy stop, stau and Higgs masses are somewhat sensitive to the values of a_i and c_i . They depend on a_i and c_i either through their boundary values at M_{GUT} , or through their RG evolutions, or through the mass-mixing induced by the low energy A -parameters.

The effects of changing a_i and c_i on the RG evolution can be read off from the following one-loop RG equations for the Higgs and third generation sfermion mass-squares:

$$\begin{aligned}
 16\pi^2 \frac{d}{dt} m_{H_u}^2 &= 3X_t - 6g_2^2 |M_2|^2 - \frac{6}{5} g_1^2 |M_1|^2, \\
 16\pi^2 \frac{d}{dt} m_{H_d}^2 &= 3X_b + X_\tau - 6g_2^2 |M_2|^2 - \frac{6}{5} g_1^2 |M_1|^2, \\
 16\pi^2 \frac{d}{dt} m_{Q_3}^2 &= X_t + X_b - \frac{32}{3} g_3^2 |M_3|^2 - 6g_2^2 |M_2|^2 - \frac{2}{15} g_1^2 |M_1|^2, \\
 16\pi^2 \frac{d}{dt} m_{U_3}^2 &= 2X_t - \frac{32}{3} g_3^2 |M_3|^2 - \frac{32}{15} g_1^2 |M_1|^2,
 \end{aligned}$$

$$\begin{aligned}
 16\pi^2 \frac{d}{dt} m_{L_3}^2 &= X_\tau - 6g_2^2 |M_2|^2 - \frac{3}{5} g_1^2 |M_1|^2, \\
 16\pi^2 \frac{d}{dt} m_{E_3}^2 &= 2X_\tau - \frac{24}{5} g_1^2 |M_1|^2,
 \end{aligned}
 \tag{3.4}$$

where

$$\begin{aligned}
 X_t &= 2y_t^2 (m_{H_u}^2 + m_{Q_3}^2 + m_{U_3}^2 + A_{H_u Q_3 U_3}^2), \\
 X_b &= 2y_b^2 (m_{H_d}^2 + m_{Q_3}^2 + m_{D_3}^2 + A_{H_d Q_3 D_3}^2), \\
 X_\tau &= 2y_\tau^2 (m_{H_d}^2 + m_{L_3}^2 + m_{E_3}^2 + A_{H_d L_3 E_3}^2).
 \end{aligned}
 \tag{3.5}$$

These RG equations show that smaller X_I ($I = t, b, \tau$) increase the low energy soft mass-squares. Since a_i and c_i determine the modulus-mediated trilinear A parameters and soft mass-squares at M_{GUT} as $\tilde{A}_{ijk} = (a_i + a_j + a_k)M_0$ and $\tilde{m}_i^2 = c_i M_0^2$, smaller $a_H = c_H$ give smaller X_I without affecting the boundary values of squark and slepton masses at M_{GUT} , eventually making the stop and stau masses at TeV scale larger. On the other hand, the consequence of smaller $a_M = c_M$ is more complicate as it depends on the relative importance of the Yukawa-induced RG evolution. It turns out that changing $a_M = c_M$ to smaller value makes the stop mass larger, while the stau mass smaller.

In Figs. 3.b and 4.b, we depict the results for the case in which $a_i = c_i = 1/2$ for both the matter and Higgs multiplets. As can be understood from the above discussion, this intermediate scale mirage mediation does not contain any parameter region of stop LSP, while having a larger parameter region of stau LSP (see Fig. 4.b). Another important feature is that the weak scale value of $|m_{H_u}^2|$ becomes smaller compared to the case of $a_i = c_i = 1$, which is mainly due to smaller X_t . This results in smaller μ and m_A . Smaller μ makes the neutralino LSP have a sizable Higgsino component, while smaller m_A makes the pseudo-scalar resonance region disappear. Again the magenta region in Fig. 3.b corresponds to the parameter region giving the WMAP DM density (3.3) under the assumption of pure thermal production. In this case, the neutralino pair annihilation into gauge boson pair becomes efficient due to the enhanced Higgsino component of neutralino LSP. Finally, the brown region is excluded by giving the $\text{Br}(b \rightarrow s\gamma)$ smaller than the allowed range.

Figs. 3.c and 4.c are the result for the case with $a_M = c_M = 1$ and $a_H = c_H = 0$, while Figs. 3.d and 4.d are for the case with $a_M = c_M = 1/2$ and $a_H = c_H = 0$. The case of $a_M = c_M = 1/2$ and $a_H = c_H = 0$ is quite similar to the case of $a_i = c_i = 1/2$: LSP is the lightest neutralino with a sizable Higgsino component for $\tan\beta \lesssim 20$ (see Figs. 4.b and 4.d). On the other hand, the case of $a_M = c_M = 1$ and $a_H = c_H = 0$ is somewhat distinctive since there is no parameter region of stop or stau LSP and the WMAP DM density is obtained for a light neutralino mass $m_{\chi^0} \sim 250$ GeV, while in other cases the WMAP DM density is obtained for heavier $m_{\chi^0} \gtrsim 350$ GeV. Again, the brown region is excluded by giving the $\text{Br}(b \rightarrow s\gamma)$ smaller than the allowed range.

3.2 Dark matter detections

If neutralino LSP is the main component of the matter budget in the Milky Way, it might be detected through the elastic scattering with terrestrial nuclear target [33, 2]. In the MSSM,

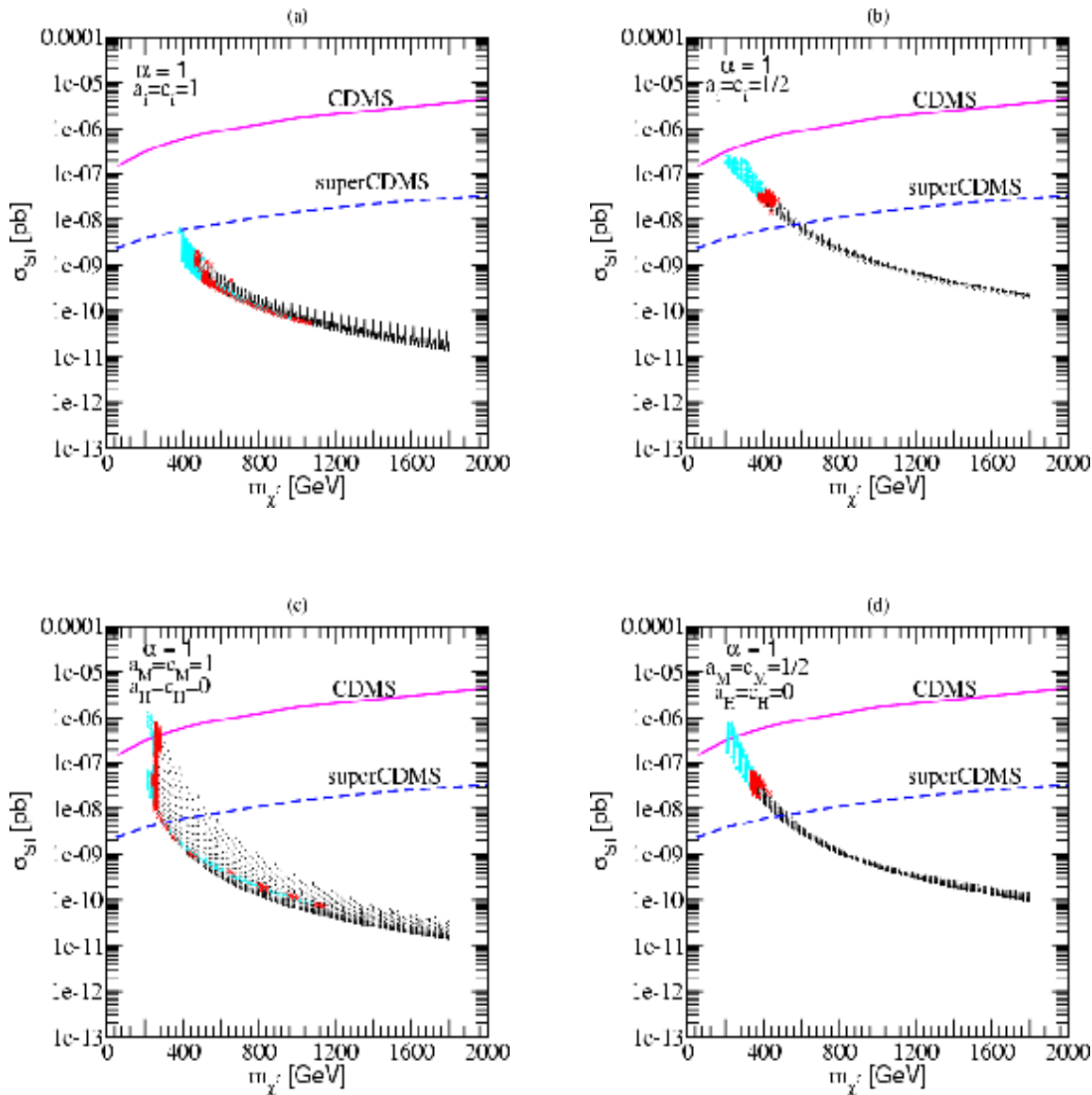


Figure 6: Scatter plot of the spin-independent neutralino-proton scattering cross section vs. m_χ in intermediate scale mirage mediation with (a_i, c_i) specified in Eq. (3.2).

t -channel Higgs boson and s -channel squark exchange processes contribute to the spin-independent (scalar) scattering between neutralino and nuclei. In many cases, dominant contribution to the scalar cross section comes from the Higgs exchange process which becomes bigger for larger $\tan\beta$, smaller Higgs masses, and mixed Bino-Higgsino LSP.

In the specific intermediate scale mirage mediation model with $a_i = c_i = 1$, the neutralino LSP is Bino-like and the mass of heavy CP-even Higgs boson is rather large when we require the neutralino to be LSP. It is thus expected that the elastic scattering cross section between neutralino DM and nuclei is rather small. In Fig. 6.a, we depict spin-independent (scalar) cross section σ_{SI} of neutralino-proton scattering as a function of the LSP neutralino mass in this specific intermediate scale mirage mediation. Here we have im-

posed the experimental bounds on the Higgs/sparticle masses and $b \rightarrow s\gamma$ branching ratio, and required that the lightest neutralino is the LSP. Red points in the figure correspond to the parameter values giving the WMAP DM density (3.3) under the assumption of pure thermal production, while the cyan points represent the parameter values for which the thermal production mechanism gives a smaller relic density. As expected, the cross section in the case of $a_i = c_i = 1$ is quite small: $\sigma_{SI} \lesssim 5 \times 10^{-9}$ pb, which is much smaller than the current experimental upper bound. It is even smaller than the sensitivity of future experiment such as SuperCDMS [34] which would reach near 10^{-9} pb level. On the other hand, intermediate scale mirage mediations with different values of (a_i, c_i) have a quite better prospect for direct detection. As can be seen from Fig. 6, most of the (red) WMAP points are above the sensitivity of SuperCDMS for the other three cases of different (a_i, c_i) . This is mainly due to the enhanced Higgsino component of the neutralino LSP and the reduced Higgs mass.

Let us now examine gamma ray signals from DM annihilation in the galactic center, providing another feasible but indirect detection method for dark matter. The integrated gamma ray flux depends on the quantity $\bar{J}(\Delta\Omega)$, which is a measure of the cuspieness of the galactic halo density profile over a spherical region of solid angle $\Delta\Omega$. In this paper, we use a conservative galactic halo model (isothermal halo density profile) which gives $\bar{J} \sim 30$ with the detector angular resolution $\Delta\Omega = 10^{-3}$ sr and set $E_{thr} = 1$ GeV for gamma ray energy threshold. Fig. 7 shows continuum gamma ray flux from the galactic center in intermediate scale mirage mediation scenarios under consideration, where red points give the WMAP value (3.3) of the relic DM density. Here the four different choices of $a_i = c_i$ do not lead to a dramatic difference in the gamma ray flux. The maximal value of flux given by the most favored WMAP (red) points is about $\text{few} \times 10^{-11} \text{cm}^{-2} \text{s}^{-1}$ which is somewhat below the expected reach ($\sim 10^{-10} \text{cm}^{-2} \text{s}^{-1}$) of GLAST, although the (cyan) points giving smaller relic density can give a larger flux around $10^{-10} \text{cm}^{-2} \text{s}^{-1}$. However, it should be noticed that our calculation for the gamma ray flux is based on a conservative halo density profile. If one uses an extreme halo model like the spiked profile [35], the resulting gamma ray flux increases by a factor of $\sim 10^4$. In this case, the gamma ray signals can be detected for a significant portion of the parameter space. A caveat is that the continuum gamma ray signals suffer from unknown astrophysical background. Recent observations of a bright gamma ray source in the direction of galaxy center by the Air Cherenkov Telescopes such as H.E.S.S. [36] might be explained by an astrophysical process rather than the dark matter annihilation [37].

We finally notice an interesting enhancement of the gamma ray flux due to the Higgs resonance effect. Fig. 8 shows the gamma ray flux from the galactic center as a function of $\tan\beta$ in the specific intermediate scale mirage mediation with $a_i = c_i = 1$ and $M_0 = 800$ GeV. One can see a clear enhancement of the flux around $\tan\beta \sim 22$ for which $m_A \sim 2m_\chi$. In this case, neutralino annihilation to heavy quarks is dominated and the subsequent quark hadronization produces many gamma rays.

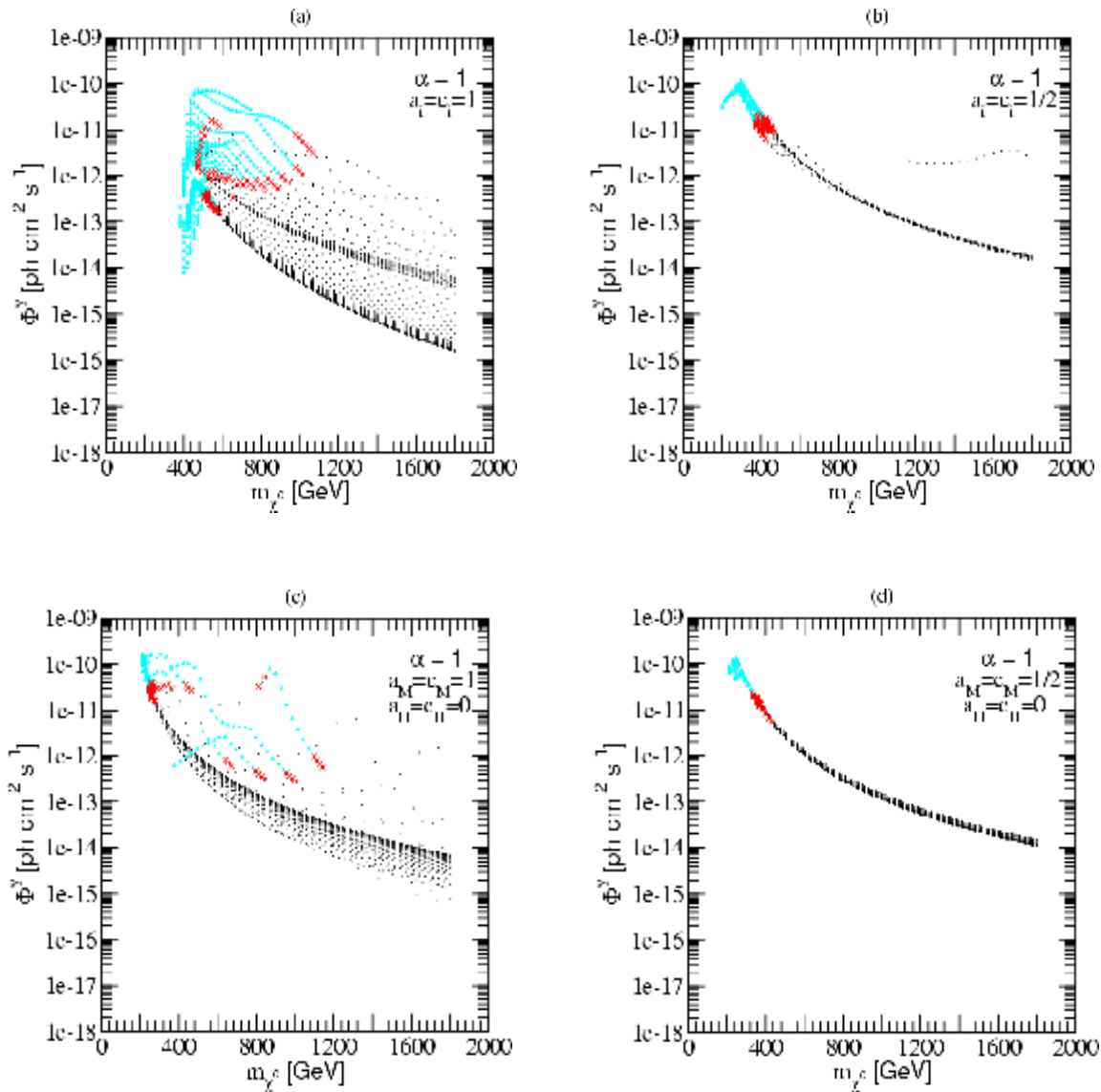


Figure 7: Scatter plot of the continuum gamma ray flux vs. m_χ in intermediate scale mirage mediation with (a_i, c_i) specified in Eq. (3.2).

4. Neutralino DM for generic mirage messenger scale

In the previous section, we have examined the prospect of neutralino DM in intermediate scale mirage mediation models ($\alpha = 1$). As was discussed in section 2, in string compactifications with non-trivial dilaton-modulus mixing, the anomaly to modulus mediation ratio α can have a more variety of values. In fact, the nature of neutralino LSP is somewhat sensitive to the value of α , typically it changes from Bino-like to Higgsino-like via Bino-Higgsino mixing region when α is increased from zero to a value of order unity. This feature is essentially due to the following behavior of the gaugino masses as a function of α :

$$M_3 : M_2 : M_1 \simeq (1 - 0.3\alpha)g_3^2 : (1 + 0.1\alpha)g_2^2 : (1 + 0.66\alpha)g_1^2, \quad (4.1)$$

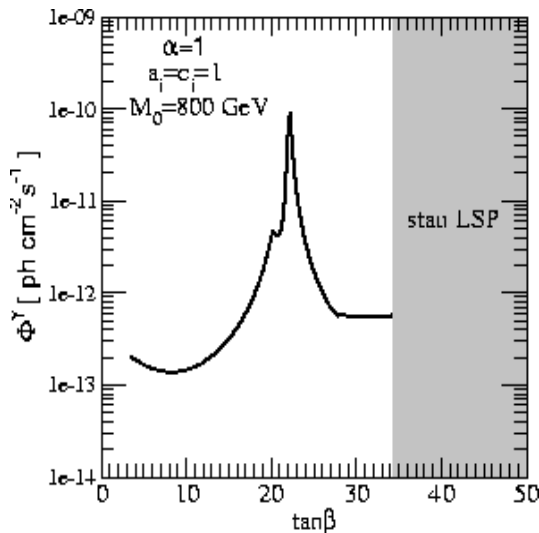


Figure 8: Continuum gamma ray flux as a function of $\tan\beta$ in the intermediate scale mirage mediation with $a_i = c_i = 1$ and $M_0 = 800$ GeV. Note the resonant peak due to the pseudo-scalar Higgs resonance.

If α increases from zero, the gluino mass decreases as $M_3 \propto (1 - 0.3\alpha)$. Smaller M_3 then weakens the radiative electroweak symmetry breaking mechanism as it gives a smaller stop mass-square, thus leads to smaller $|m_{H_u}|^2$ and $|\mu|$ at the weak scale. On the other hand, the Bino mass increases as $M_1 \propto (1 + 0.66\alpha)$, thus the lightest neutralino changes from Bino-like to Higgsino-like when α is varying from zero to a positive value of order unity. If α is further increased, eventually the model does not allow electroweak symmetry breaking. In this section, we extend the analysis of the previous section to the range of α from zero to the value at which the electroweak symmetry starts to be restored.

4.1 Parameter region of neutralino LSP and thermal relic Density

Again, let us first consider the case with $a_i = c_i = 1$. We will treat M_0 and α as free parameters, while focusing on $\tan\beta = 10$ and 35 . Figs. 9.a and 9.b show how some of the superparticle masses vary as a function of α for a fixed $M_0 = 800$ GeV. For $\alpha \lesssim 1$, the LSP is the lightest neutralino which is mostly Bino, and thus its mass varies as $m_{\chi^0} \simeq M_1 \propto (1 + 0.66\alpha)$. In the range of $1 \lesssim \alpha \lesssim 1.8$, stau or stop becomes the LSP. For $1.8 \lesssim \alpha \lesssim 2$, the lightest neutralino which is now mostly Higgsino becomes the LSP. If α increases further, the model does not allow electroweak symmetry breaking.

In Figs. 9.c and 9.d, the two distinct magenta regions separated by stop/stau LSP regions give the WMAP DM density, $0.085 < \Omega_{DM} h^2 < 0.119$, under the assumption that all neutralino DMs are produced by the conventional thermal production mechanism. Below (above) these magenta regions, $\Omega_{\chi} h^2 < 0.085$ (> 0.119). In the Bino-like LSP region, stop-neutralino coannihilation plays a crucial role to get the WMAP DM density for $\tan\beta = 10$, while stau-neutralino coannihilation or pseudoscalar Higgs resonance processes are important for $\tan\beta = 35$. For Higgsino-like LSP, the charged Higgsino χ_1^\pm and two neutral Higgsinos χ_1^0, χ_2^0 are nearly degenerate. Then the dominant annihilation processes

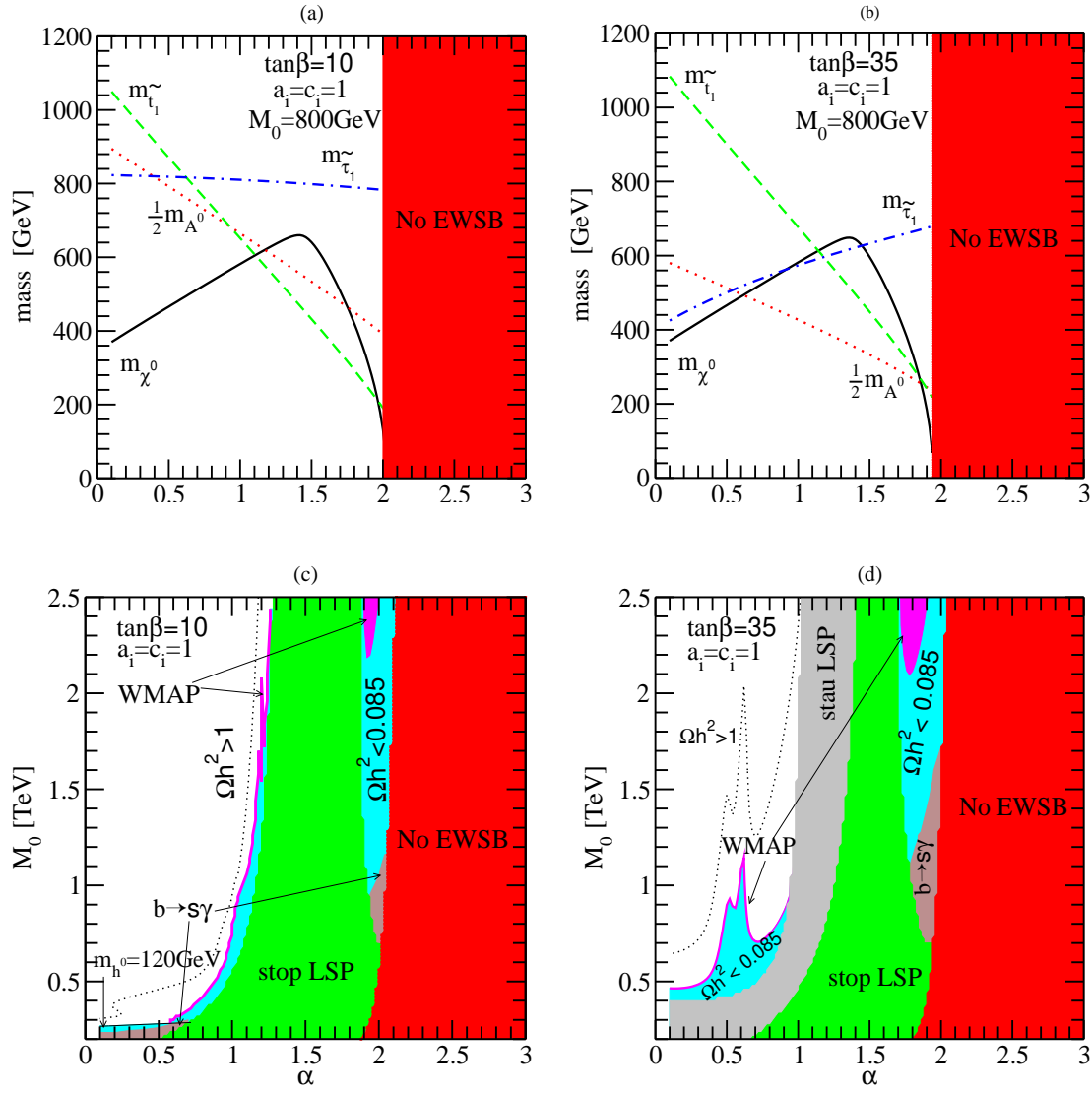


Figure 9: Sparticle masses vs. α for $\tan\beta = 10$ and $\tan\beta = 35$ in case with $a_i = c_i = 1$. The lower figures show the parameter space of neutralino LSP and its thermal relic density on the plane of (α, M_0) .

are the neutralino pair annihilation into gauge bosons, and the neutralino-chargino co-annihilation into fermion pair [38]. These annihilations of Higgsino-like LSP are very efficient, so that the relic mass density is too small unless m_{χ^0} is quite heavy. Indeed, from Figs. 9.c and 9.d, we can see that the WMAP DM density is obtained only for $M_0 \gtrsim 2.2$ TeV in the Higgsino LSP region around $\alpha \sim 1.8$. However it should be stressed that the cyan regions of Figs. 9.c and 9.d can be allowed if some part of DM were produced by non-thermal mechanism. Such parameter region contains $\alpha \sim 1.8$ and $M_0 \sim 1$ TeV for which the neutral Higgsino with $m_{\chi^0} \sim 200$ GeV is the LSP and the stop is rather light as $m_{\tilde{t}_1} \sim 250$ GeV. The brown regions are excluded by the $b \rightarrow s\gamma$ constraint. On the brown region in Fig. 9.c, the chargino loop contribution to $b \rightarrow s\gamma$ dominates, which results in

$\text{Br}(b \rightarrow s\gamma)$ smaller than the experimentally allowed range.

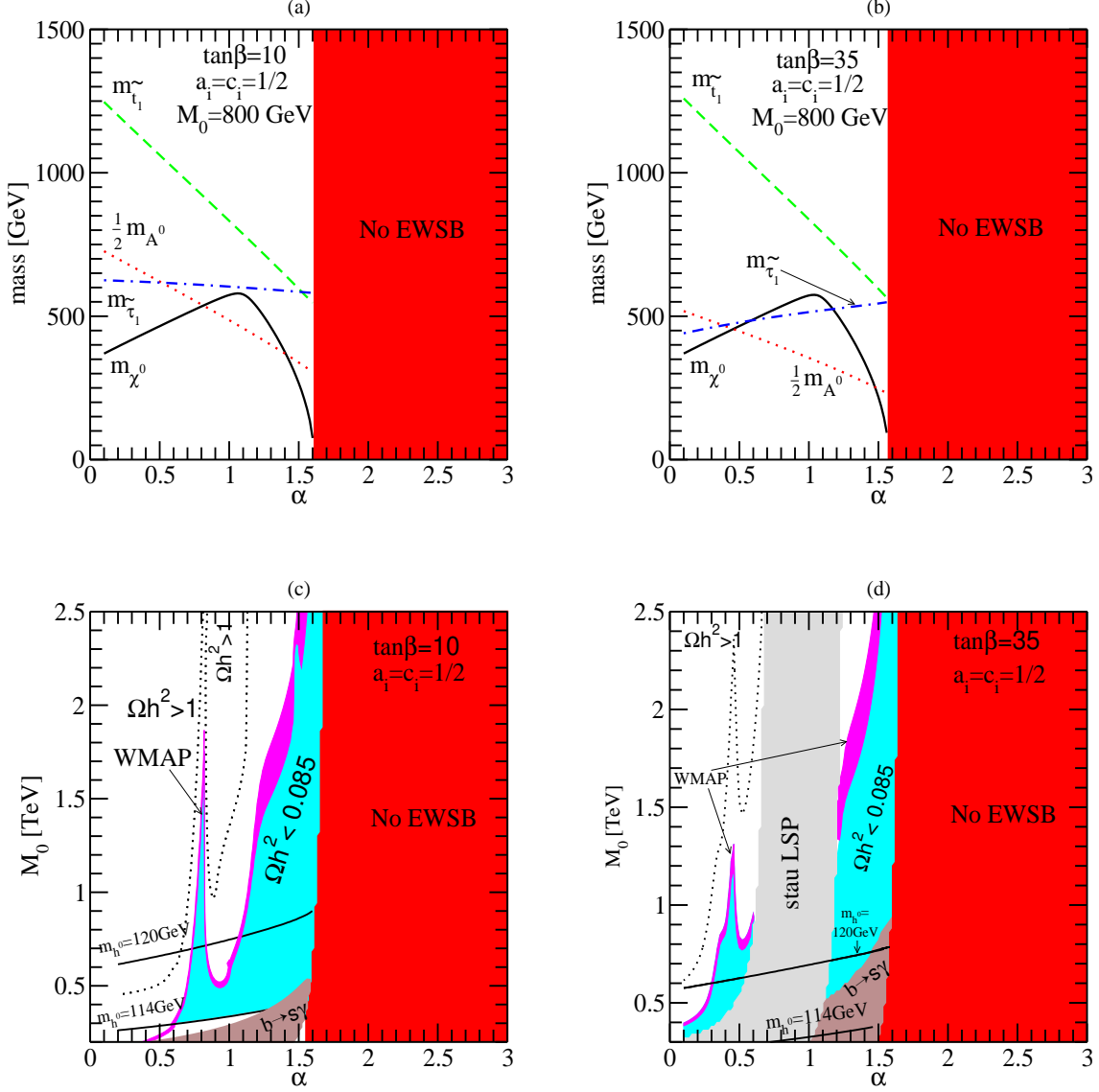


Figure 10: The results for the case in which $a_i = c_i = 1/2$ for both the Higgs and matter multiplets.

Let us now consider the case with $a_i = c_i = 1/2$. Obviously, smaller (a_i, c_i) give smaller stop/stau mass-squares at M_{GUT} . However, as was anticipated in the previous section, X_I ($I = t, b, \tau$) which govern the RG evolution of stop/stau mass-squares (see Eq. 3.4) become smaller also, which would increase the stop/stau masses at the weak scale. Together with the reduction of $A_{H_u Q_3 U_3}$, this effect on the RG evolution eventually makes the physical lighter stop mass $m_{\tilde{t}_1}$ larger compared to the case with $a_i = c_i = 1$. On the other hand, stau masses are more affected by the change of the boundary values, thus their weak scale values become lighter compared to the case of $a_i = c_i = 1$. Smaller X_t leads to also a

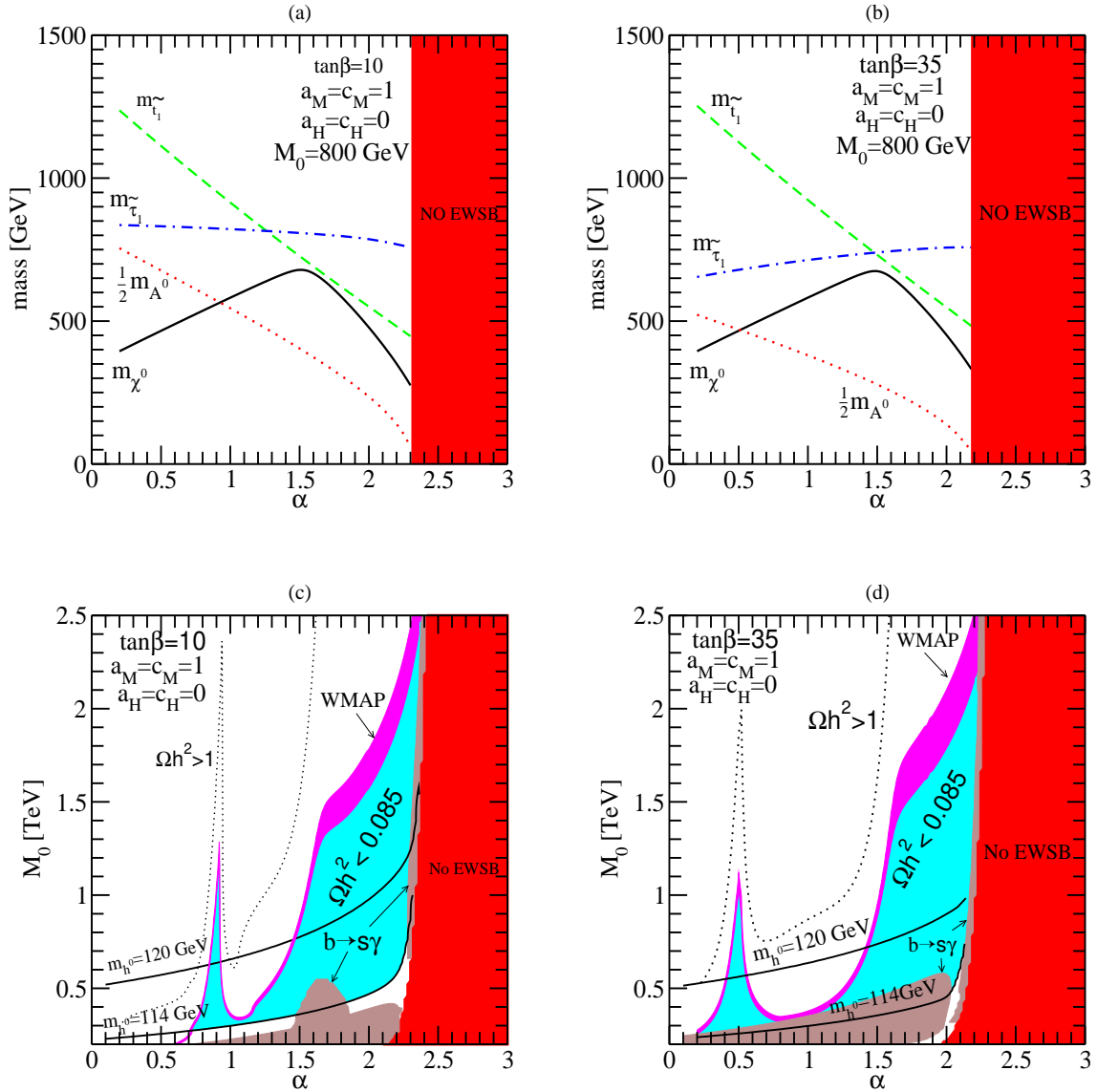


Figure 11: The results for the case in which $a_H = c_H = 0$ and $a_M = c_M = 1$.

smaller $|m_{H_u}^2|$ at the weak scale, resulting the reduction of the Higgsino mass μ and the pseudoscalar Higgs boson mass m_A . Figs. 10.a and 10.b show all of these features. Again, as α increases, the neutralino LSP changes from Bino-like to Higgsino-like. Comparing to Fig. 9, the lighter stop becomes heavier, while the lighter stau and the pseudoscalar Higgs become lighter. As a consequence, the stop LSP region disappears, but the stau LSP region at large $\tan\beta$ becomes larger. The magenta regions of Figs. 10.c and 10.d correspond to the parameter region giving the WMAP DM density under the assumption of pure thermal production. They clearly show the Higgsino-like LSP at $\alpha > 1$ and also the pseudoscalar Higgs resonance effect for the Bino-like LSP at smaller α .

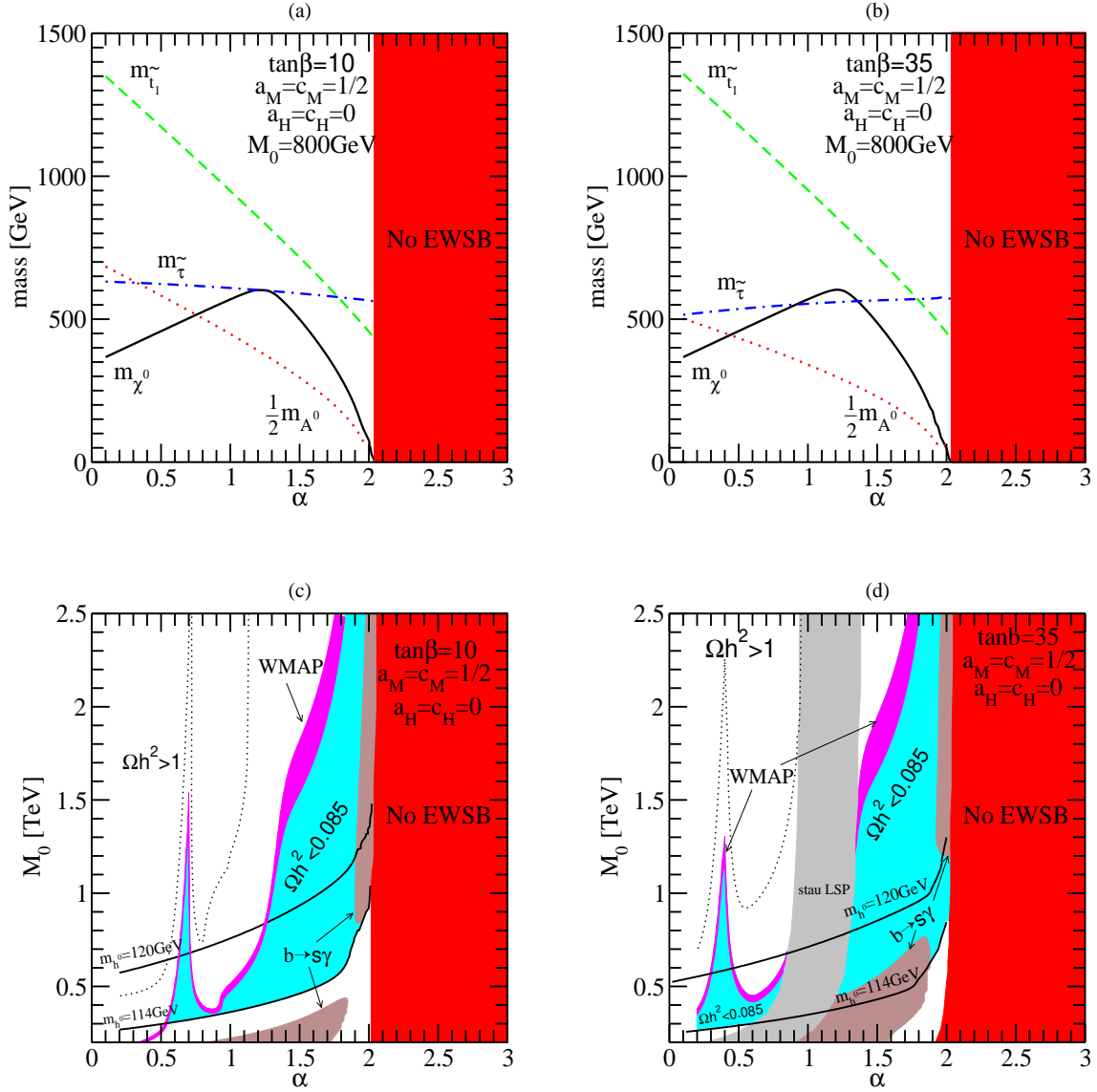


Figure 12: The results for the case in which $a_H = c_H = 0$ and $a_M = c_M = 1/2$.

Fig. 11 shows the results for the case in which $a_H = c_H = 0$ for the Higgs multiplets, while $a_M = c_M = 1$ for the quark/lepton matter multiplets. A characteristic feature of this case is that the lightest neutralino is the LSP over the entire region of parameter space allowing the electroweak symmetry breaking. Compared to the case in which $a_i = c_i = 1$ for both the Higgs and matter multiplets, X_I ($I = t, b, \tau$) for the RG evolution (3.4) have smaller values, while the boundary values of stop/stau mass-squares remain the same. This results in heavier stop and stau at the weak scale. Except for the absence of stop/stau LSP region, other features are somewhat similar to other cases. The brown regions are excluded by the $b \rightarrow s\gamma$ constraint. On the brown region with small M_0 in Fig. 11.c, the chargino loop contribution to $b \rightarrow s\gamma$ dominates, which results in $\text{Br}(b \rightarrow s\gamma)$ smaller than the experimentally allowed range. On the other hand, the charged Higgs boson loop

becomes significant in the large M_0 region, making the predicted $\text{Br}(b \rightarrow s\gamma)$ exceed the experimental bound. The region between those two brown regions is allowed due to the cancellation between the chargino and charged Higgs boson loop contributions.

Finally, Fig. 12 is for the case with $a_H = c_H = 0$ and $a_M = c_M = 1/2$. The results are quite similar to the case in which $a_i = c_i = 1/2$ for both the Higgs and matter multiplets. The $\alpha = 2$ region of this case corresponds to the TeV scale mirage mediation model proposed in [30] as a model to minimize the fine tuning for the electroweak symmetry breaking in the MSSM.

4.2 Dark matter detections

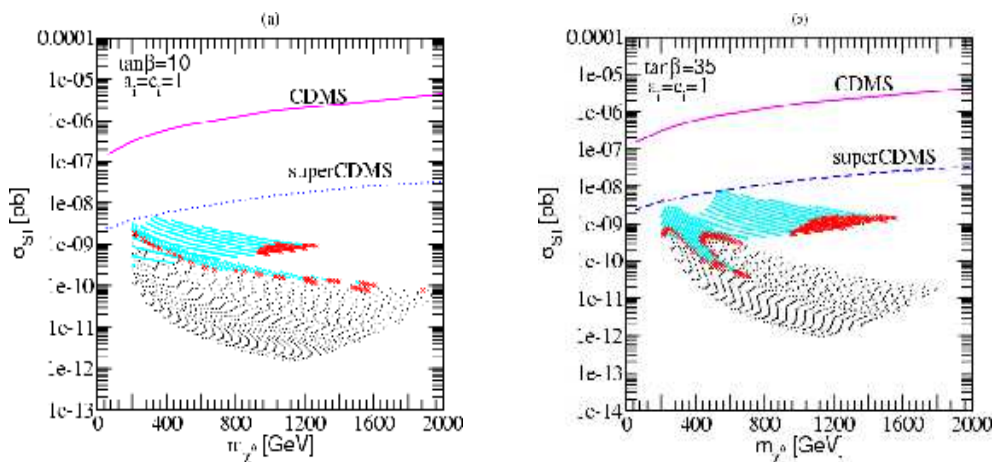


Figure 13: Spin-independent neutralino and proton scattering cross section in case with $a_i = c_i = 1$.

To see the prospect of direct DM detection, spin-independent cross section of the neutralino-proton scattering is presented in Fig. 13 for the case with $a_i = c_i = 1$. Here, we imposed the experimental bounds on sparticle and Higgs masses, and $b \rightarrow s\gamma$ branching ratio. In the figures, the red points give the WMAP DM density: $0.085 < \Omega_\chi h^2 < 0.119$, the cyan corresponds to the region giving $\Omega_\chi h^2 < 0.085$, and the rest gives $\Omega_\chi h^2 > 0.119$, under the assumption of pure thermal production of neutralino DM. One can notice that there are two distinct branches of the WMAP points which correspond to the Bino branch and the Higgsino branch, respectively. In our scan, Higgsino-like LSP gives a larger σ_{SI} for a given m_χ . The dominant contribution to σ_{SI} usually comes from the Higgs exchange process which becomes significant if the LSP neutralino is a mixed Bino-Higgsino state. On the other hand, for $a_i = c_i = 1$, the LSP neutralino is either Bino-like or Higgsino-like since the mixed Bino-Higgsino region gives a stop or stau LSP. Therefore, it is expected that the cross section is rather small for the case with $a_i = c_i = 1$. Indeed, Fig. 13 shows that the predicted values are all less than the current and near future experimental sensitivity.

However, the prospect of direct DM detection is dramatically changed if one considers other choices of a_i and c_i . Fig. 14 shows the predictions for spin-independent cross section of

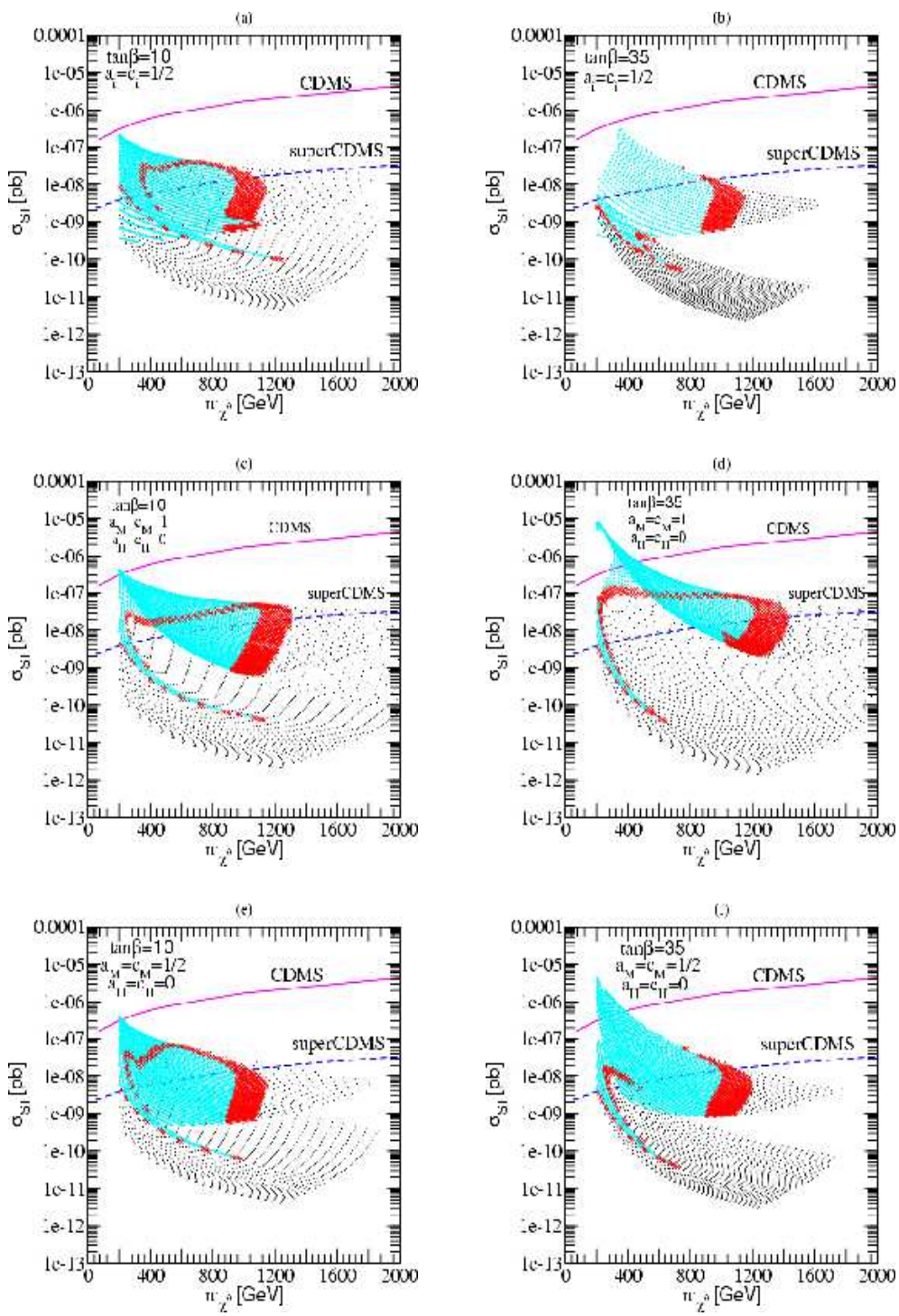


Figure 14: Spin-independent neutralino and proton scattering cross section for other values of (a_i, c_i) giving a mixed Bino-Higgsino LSP over a significant fraction of the parameter space.

the neutralino-proton scattering for the three other choices of (a_i, c_i) giving a mixed Bino-Higgsino LSP over a significant fraction of the parameter space and also a reduced value

of the pseudoscalar Higgs mass. These values of a_i and c_i give heavier stop, thereby the $b \rightarrow s\gamma$ constraint becomes less significant compared to the case with $a_i = c_i = 1$. Again, the red points represent the parameter values giving the WMAP DM density $0.085 < \Omega_\chi h^2 < 0.119$, the cyan points give $\Omega_\chi h^2 < 0.085$, and the rest stands for $\Omega_\chi h^2 > 0.119$, under the assumption of thermal production of neutralino LSP. As expected, the scattering cross sections are largely enhanced compared to the case with $a_i = c_i = 1$. Now, much of the WMAP points give σ_{SI} exceeding the sensitivity limit of the planned SuperCDMS experiment. If one includes the cyan points, the cross section can be much bigger, reaching even at the current CDMS sensitivity limit.

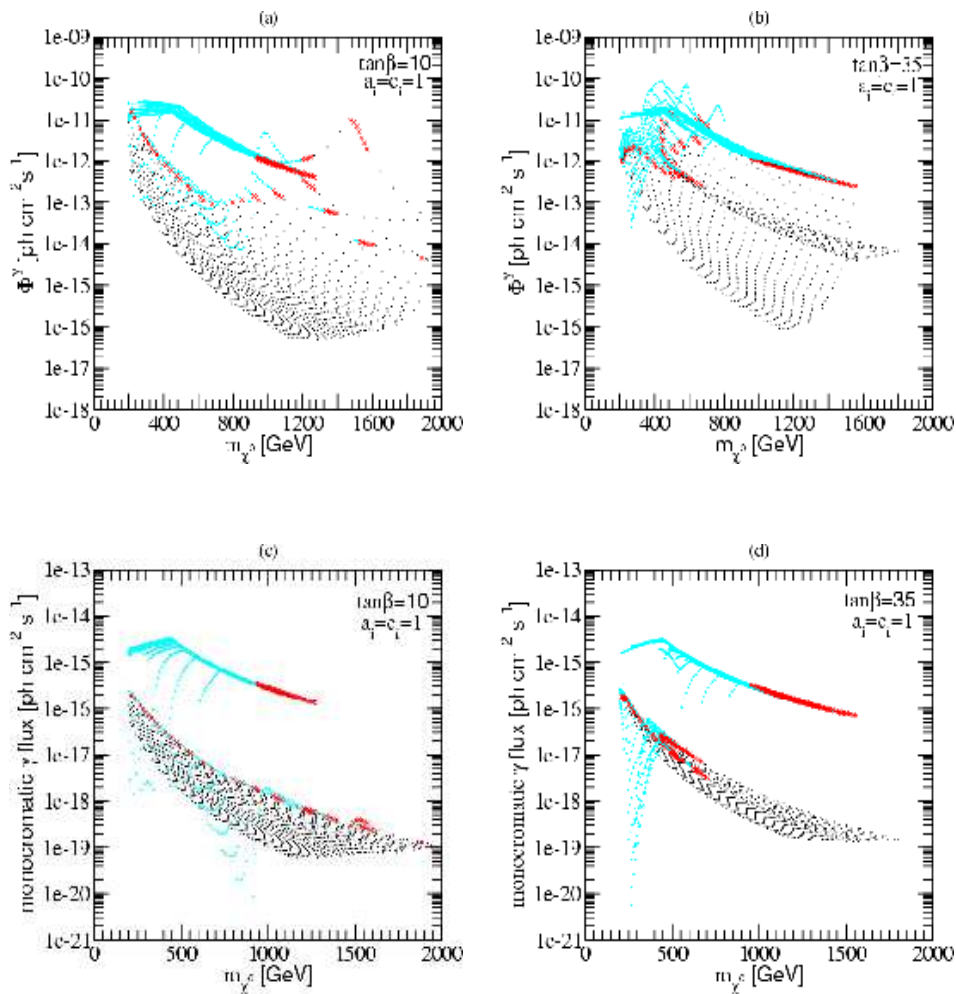


Figure 15: Continuum (a and b) and monochromatic (c and d) gamma ray flux from the Galactic Center vs. m_χ for the case with $a_i = c_i = 1$ and $\tan\beta = 10$ or 35 .

Gamma rays induced by neutralino annihilation in Galactic Center might provide an indirect detection of neutralino DM. Fig. 15 shows the predicted continuum (a and b) and monochromatic (c and d) gamma ray fluxes from the Galactic Center as a function of the LSP neutralino mass for the case with $a_i = c_i = 1$. Here we chose the same halo density profile as the previous section, giving $\bar{J}(\Delta\Omega = 10^{-3}\text{sr}) \sim 30$. The red points in

the figures give the WMAP DM density, while the cyan and the rest give $\Omega_\chi h^2 < 0.085$ and $\Omega_\chi h^2 > 0.119$, respectively, under the assumption of pure thermal production. Again the WMAP points have two distinct branches, the Bino-branch and the Higgsino-branch. Including the cyan points giving smaller thermal relic DM density, the case with $a_i = c_i$ can give a continuum gamma ray flux up to $2 \times 10^{-11} \text{cm}^{-2} \text{s}^{-1}$ and $10^{-10} \text{cm}^{-2} \text{s}^{-1}$ for $\tan \beta = 10$ and 35, respectively. This maximum flux of the continuum gamma rays barely touch the expected reach of GLAST. However, the real gamma ray flux can be much bigger than these predictions if the actual halo density profile is denser than the assumed profile. For Higgsino LSP, unsuppressed annihilation into W or Z boson pair is the major source of continuum gamma rays. As can be noticed from Fig. 15, for some parameter values, the gamma ray flux from Bino LSP is largely enhanced by the pseudoscalar Higgs resonance effect.

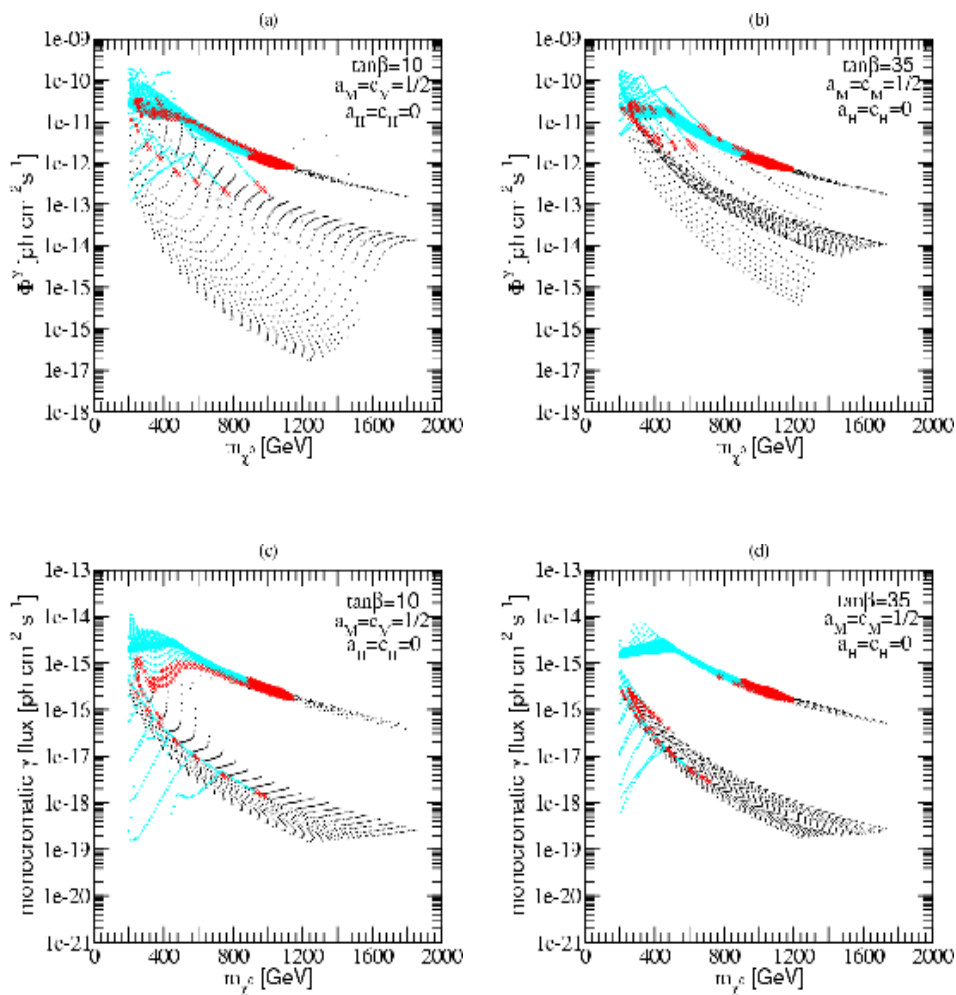


Figure 16: Continuum (a and b) and monochromatic (c and d) gamma ray flux from the Galactic Center vs. m_χ for the case in which $a_H = c_H = 0$, $a_M = c_M = 1/2$, and $\tan \beta = 10$ or 35.

In fact, it is quite nontrivial to discriminate the continuum gamma rays produced by neutralino annihilation from the diffuse galactic gamma ray backgrounds. On the other

hand, the monochromatic gamma ray line from $\chi\chi \rightarrow \gamma\gamma$ or γZ can be considered as a 'smoking gun' signal of WIMP dark matter. Figs. 15.c and 15.d show the gamma ray line flux produced by neutralino pair annihilation in Galactic Center for the case with $a_i = c_i$. One can notice that there is a clear distinction between the Bino and Higgsino LSP regions. The gamma ray line flux ranges from 10^{-19} to $10^{-16} \text{ cm}^{-2}\text{s}^{-1}$ for the Bino LSP branch of WMAP points, while it ranges from 10^{-16} to $10^{-15} \text{ cm}^{-2}\text{s}^{-1}$ for the Higgsino LSP branch. For Higgsino-like LSP, the gamma ray line flux comes dominantly from the $W^\pm\chi_1^\mp$ loop diagrams resulting in a large cross section for $\chi\chi \rightarrow \gamma\gamma$ or γZ [39]. While GLAST will probe the photon energies only up to 300 GeV with a low energy threshold, Atmospheric Cherenkov Telescopes (ACT) such as H.E.S.S. will be able to cover higher photon energy ranges and probe the gamma ray flux down to $10^{-14} \text{ cm}^{-2}\text{s}^{-1}$. The predicted monochromatic fluxes in Figs. 15.c and 15.d are still below this sensitivity limit. However, as we have stressed, these results are based on a rather conservative halo density profile. In view of that the predicted flux can increase even by a factor of 10^4 if one uses an extreme halo model like the spiked profile, the monochromatic gamma ray signal for the Higgsino dark matter might be measurable in case of a cuspy halo density profile.

As we have anticipated, other values of (a_i, c_i) specified in (3.2) allow a mixed Bino-Higgsino LSP over a significant fraction of parameter space. It is thus expected that those other cases can give a larger gamma ray flux compared to the case with $a_i = c_i = 1$. In Fig. 16, we depicted the results for the case with $a_H = c_H = 0$ and $a_M = c_M = 1/2$. Indeed, this case gives a larger flux, although not dramatically different. The red WMAP points can give a continuum gamma ray flux up to $3 \times 10^{-11} \text{ cm}^{-2}\text{s}^{-1}$, while the cyan points giving smaller thermal relic DM density can reach up to $2 \times 10^{-10} \text{ cm}^{-2}\text{s}^{-1}$. The maximal flux of monochromatic gamma ray is about $10^{-15} \text{ cm}^{-2}\text{s}^{-1}$ for the red WMAP points and about $7 \times 10^{-15} \text{ cm}^{-2}\text{s}^{-1}$ for the cyan points. Again, these results are obtained for the conservative halo density profile giving $\bar{J}(\Delta\Omega = 10^{-3}\text{sr}) \sim 30$. The real gamma ray flux can be significantly bigger than these predictions if the actual halo density profile is denser than the assumed profile.

5. Conclusions

In this paper, we have examined the prospect of neutralino dark matter in mirage mediation scenario of SUSY breaking in which soft masses receive comparable contributions from modulus mediation and anomaly mediation. Depending upon the model parameters, especially the anomaly to modulus mediation ratio, the nature of the lightest neutralino changes from Bino-like to Higgsino-like via Bino-Higgsino mixing region. For Bino-like LSP, the conventional thermal production mechanism can give a right amount of relic DM density, i.e. the WMAP observation $0.085 < \Omega_{DM}h^2 < 0.119$, through the stop/stau-neutralino coannihilation process or the pseudo-scalar Higgs resonance effect. In overall, compared to the mSUGRA scenario, a significantly larger fraction of the parameter space can give the WMAP DM density under the assumption of thermal production, while satisfying all known phenomenological constraints. This is partly because the lightest neutralino is a mixed Bino-Higgsino over a sizable fraction of the parameter space.

We also studied the detection possibilities of neutralino dark matter in mirage mediation. For the parameter region giving the WMAP density of Bino-like or Higgsino-like LSP, direct detection via elastic scattering between neutralino DM and nuclear target turns out to be mostly under the sensitivity of near future experiments. However the other parameter region giving the WMAP density of mixed Bino-Higgsino LSP predicts typically a cross section above the expected sensitivity limit of SuperCDMS. The continuum and monochromatic gamma ray fluxes from neutralino annihilation in Galactic Center have been analyzed also. Generically, Higgsino-like LSP gives a larger gamma ray flux than Bino-like LSP, however the continuum gamma ray flux from Bino LSP can be significantly enhanced for some particular parameter values due to the pseudo-scalar Higgs resonance effect. Although the gamma ray fluxes predicted within a conservative halo model are below the sensitivity of ongoing and planned experiments, it might be detectable if the actual halo density is denser than the conservative profile used in our analysis.

Acknowledgments

We thank Kwang-Sik Jeong for helpful discussions and also for clarifying various conventions for soft terms. This work is supported by the KRF Grant KRF-2005-201-C00006 funded by the Korean Government (K.C. and Y.S.), the KOSEF Grant R01-2005-000-10404-0 (K.C. and Y.S.), the Center for High Energy Physics of Kyungpook National University (K.C.), the BK21 program of Ministry of Education (K.Y.L.), and the Astrophysical Research Center for the Structure and Evolution of the Cosmos funded by the KOSEF (Y.G.K.). K.O. has been supported by the grant-in-aid for scientific research on priority areas (No. 441): "Progress in elementary particle physics of the 21 century through discoveries of Higgs boson and supersymmetry" (No. 16081209) from the Ministry of Education, Culture, Sports, Science and Technology of Japan. K.O. and Y.S. thank Yukawa Institute in Kyoto University for the use of Altix3700 BX2 by which much of the numerical calculation has been made. Y.S. also thanks the Particle Theory and Cosmology Group at Tohoku University for the use of the computer facility.

Appendix A.

In this appendix, we summarize the notations and conventions used in this paper. The quantum effective action in $N = 1$ superspace is given by

$$\begin{aligned}
 & \int d^4\theta \left[-3CC^* e^{-K/3} + \frac{1}{16} \left(G_a W^{a\alpha} \frac{D^2}{\partial^2} W_\alpha^a + \text{h.c.} \right) \right] + \left(\int d^2\theta C^3 W + \text{h.c.} \right) \\
 = & \int d^4\theta \left[-3CC^* e^{-K_0/3} + CC^* e^{-K_0/3} Z_i \Phi_i^* e^{2V_a T_a} \Phi_i + \frac{1}{16} \left(G_a W^{a\alpha} \frac{D^2}{\partial^2} W_\alpha^a + \text{h.c.} \right) \right] \\
 & + \left(\int d^2\theta C^3 \left[W_0 + \frac{1}{6} \lambda_{ijk} \Phi_i \Phi_j \Phi_k \right] + \text{h.c.} \right) + \dots, \tag{5.1}
 \end{aligned}$$

where the gauge kinetic terms are written as a D -term operator to accommodate the radiative corrections to gauge couplings, and the ellipsis stands for the irrelevant higher dimensional operators. The Kähler potential K is expanded as

$$K = K_0(T_A, T_A^*) + Z_i(T_A, T_A^*) \Phi_i^* e^{2V_a T_a} \Phi_i + \dots, \quad (5.2)$$

where V_a and Φ_i denote the visible gauge and matter superfields given by

$$\begin{aligned} \Phi^i &= \phi^i + \sqrt{2} \theta \psi^i + \theta^2 F^i, \\ V^a &= -\theta \sigma^\mu \bar{\theta} A_\mu^a - i \bar{\theta}^2 \theta \lambda^a + i \theta^2 \bar{\theta} \bar{\lambda}^a + \frac{1}{2} \theta^2 \bar{\theta}^2 D^a, \end{aligned} \quad (5.3)$$

and $T_A = (C, T)$ are the SUSY breaking messengers including the conformal compensator superfield $C = C_0 + \theta^2 F^C$ and the modulus superfield $T = T_0 + \sqrt{2} \theta \hat{T} + \theta^2 F^T$. The radiative corrections due to renormalizable gauge and Yukawa interactions can be encoded in the matter Kähler metric Z_i and the gauge coupling superfield G_a which is given by

$$G_a = \text{Re}(f_a) + \Delta G_a, \quad (5.4)$$

where f_a is the holomorphic gauge kinetic function and ΔG_a includes the T_A -dependent radiative correction to gauge coupling. The superpotential is expanded as

$$W = W_0(T) + \frac{1}{6} \lambda_{ijk}(T) \Phi_i \Phi_j \Phi_k + \dots, \quad (5.5)$$

where $W_0(T)$ is the modulus superpotential stabilizing T . Here we do not specify the mechanism to generate the MSSM Higgs parameters μ and B , and treat them as free parameters constrained only by the electroweak symmetry breaking condition. For a discussion of μ and B in mirage mediation, see Ref. [9].

For the canonically normalized component fields, the above superspace action gives the following form of the running gauge and Yukawa couplings, the supersymmetric gaugino-matter fermion coupling $\mathcal{L}_{\lambda\psi}$, and the soft SUSY breaking terms:

$$\begin{aligned} \frac{1}{g_a^2} &= \text{Re}(G_a), \quad y_{ijk} = \frac{\lambda_{ijk}}{\sqrt{e^{-K_0} Z_i Z_j Z_k}}, \\ \mathcal{L}_{\lambda\psi} &= i\sqrt{2} (\phi_i^* T^a \psi_i \lambda^a - \bar{\lambda}^a T^a \phi_i \bar{\psi}_i), \\ \mathcal{L}_{\text{soft}} &= -m_i^2 \phi^i \phi^{i*} - \left(\frac{1}{2} M_a \lambda^a \lambda^a + \frac{1}{6} A_{ijk} y_{ijk} \phi^i \phi^j \phi^k + \text{h.c.} \right), \end{aligned} \quad (5.6)$$

where

$$\begin{aligned} M_a &= F^A \partial_A \ln(\text{Re}(G_a)), \\ A_{ijk} &= -F^A \partial_A \ln \left(\frac{\lambda_{ijk}}{e^{-K_0} Z_i Z_j Z_k} \right), \\ m_i^2 &= -F^A F^{B*} \partial_A \partial_{\bar{B}} \ln \left(e^{-K_0/3} Z_i \right) \end{aligned} \quad (5.7)$$

for

$$\begin{aligned} F^T &= -e^{K_0/2} (\partial_T \partial_{T^*})^{-1} (D_T W_0)^*, \\ F^C &= m_{3/2}^* + \frac{1}{3} \partial_T K_0 F^T \quad (m_{3/2} = e^{K_0/2} W_0). \end{aligned} \quad (5.8)$$

In the approximation ignoring the off-diagonal components of $w_{ij} = \sum_{pq} y_{ipq} y_{jpp}^*$, the 1-loop RG evolution of soft parameters is determined by

$$\begin{aligned}
 16\pi^2 \frac{dM_a}{d\ln\mu} &= 2 \left[-3 \operatorname{tr} \left(T_a^2(\text{Adj}) \right) + \sum_i \operatorname{tr} \left(T_a^2(\phi^i) \right) \right] g_a^2 M_a, \\
 16\pi^2 \frac{dA_{ijk}}{d\ln\mu} &= \left[\sum_{p,q} |y_{ipq}|^2 A_{ipq} - 4 \sum_a g_a^2 C_2^a(\phi^i) M_a \right] + [i \leftrightarrow j] + [i \leftrightarrow k], \\
 16\pi^2 \frac{dm_i^2}{d\ln\mu} &= \sum_{j,k} |y_{ijk}|^2 (m_i^2 + m_j^2 + m_k^2 + |A_{ijk}|^2) \\
 &\quad - 8 \sum_a g_a^2 C_2^a(\phi^i) |M_a|^2 + 2g_1^2 q_i \sum_j q_j m_j^2,
 \end{aligned} \tag{5.9}$$

where the quadratic Casimir $C_2^a(\phi_i) = (N^2 - 1)/2N$ for a fundamental representation ϕ_i of the gauge group $SU(N)$, $C_2^a(\phi_i) = q_i^2$ for the $U(1)$ charge q_i of ϕ_i .

In mirage mediation, soft terms at M_{GUT} are determined by the modulus mediation of $\mathcal{O}(F^T/T)$ and the anomaly mediation of $\mathcal{O}(F^C/8\pi^2 C_0)$ which are comparable to each other. In the presence of the axionic shift symmetry

$$U(1)_T : \quad \operatorname{Im}(T) + \text{real constant} \tag{5.10}$$

which is broken by the non-perturbative term in the modulus superpotential

$$W_0 = w - Ae^{-aT}, \tag{5.11}$$

one can always make that $m_{3/2}$ and F^T are simultaneously real. Also since $F^T/T \sim m_{3/2}/4\pi^2$, we have

$$\frac{F^C}{C_0} = m_{3/2} \left(1 + \mathcal{O} \left(\frac{1}{8\pi^2} \right) \right). \tag{5.12}$$

Then, upon ignoring the parts of $\mathcal{O}(F^T/8\pi^2 T)$, the resulting soft parameters at M_{GUT} are given by

$$\begin{aligned}
 M_a &= M_0 + \frac{m_{3/2}}{16\pi^2} b_a g_a^2, \\
 A_{ijk} &= \tilde{A}_{ijk} - \frac{m_{3/2}}{16\pi^2} (\gamma_i + \gamma_j + \gamma_k), \\
 m_i^2 &= \tilde{m}_i^2 - \frac{m_{3/2}}{16\pi^2} M_0 \theta_i - \left(\frac{m_{3/2}}{16\pi^2} \right)^2 \gamma_i,
 \end{aligned} \tag{5.13}$$

where

$$\begin{aligned}
 M_0 &= F^T \partial_T \ln \operatorname{Re}(f_a), \\
 \tilde{A}_{ijk} &\equiv (a_i + a_j + a_k) M_0 = F^T \partial_T \ln(e^{-K_0} Z_i Z_j Z_k), \\
 \tilde{m}_i^2 &\equiv c_i M_0^2 = -|F^T|^2 \partial_T \partial_{\bar{T}} \ln(e^{-K_0/3} Z_i),
 \end{aligned} \tag{5.14}$$

and

$$\begin{aligned}
 b_a &= -3\text{tr}(T_a^2(\text{Adj})) + \sum_i \text{tr}(T_a^2(\phi_i)), \\
 \gamma_i &= 2 \sum_a g_a^2 C_2^a(\phi_i) - \frac{1}{2} \sum_{jk} |y_{ijk}|^2, \\
 \theta_i &= 4 \sum_a g_a^2 C_2^a(\phi_i) - \sum_{jk} |y_{ijk}|^2 (a_i + a_j + a_k), \\
 \dot{\gamma}_i &= 8\pi^2 \frac{d\gamma_i}{d \ln \mu},
 \end{aligned} \tag{5.15}$$

where $\omega_{ij} = \sum_{kl} y_{ikl} y_{jkl}^*$ is assumed to be diagonal. Here we have used that λ_{ijk} are T -independent constant as ensured by the axionic shift symmetry $U(1)_T$.

Let us now summarize our conventions for the MSSM. The superpotential of canonically normalized matter superfields is given by

$$W = y_D H_d \cdot Q D^c + y_L H_d \cdot L E^c - y_U H_u \cdot Q U^c - \mu H_d \cdot H_u, \tag{5.16}$$

where the $SU(2)_L$ product is $H \cdot Q = \epsilon_{ab} H^a Q^b$ with $\epsilon_{12} = -\epsilon_{21} = 1$, and color indices are suppressed. Then the chargino and neutralino mass matrices are given by

$$-\frac{1}{2} \tilde{\psi}^{-T} \mathcal{M}_C \tilde{\psi}^+ - \frac{1}{2} \tilde{\psi}^{0T} \mathcal{M}_N \tilde{\psi}^0 + \text{h.c.}, \tag{5.17}$$

where

$$\begin{aligned}
 \mathcal{M}_C &= \begin{pmatrix} -M_2 & g_2 \langle H_u^0 \rangle \\ g_2 \langle H_d^0 \rangle & \mu \end{pmatrix}, \\
 \mathcal{M}_N &= \begin{pmatrix} -M_1 & 0 & -\frac{1}{\sqrt{2}} g_Y \langle H_d^0 \rangle & \frac{1}{\sqrt{2}} g_Y \langle H_u^0 \rangle \\ 0 & -M_2 & \frac{1}{\sqrt{2}} g_2 \langle H_d^0 \rangle & -\frac{1}{\sqrt{2}} g_2 \langle H_u^0 \rangle \\ -\frac{1}{\sqrt{2}} g_Y \langle H_d^0 \rangle & \frac{1}{\sqrt{2}} g_2 \langle H_d^0 \rangle & 0 & -\mu \\ \frac{1}{\sqrt{2}} g_Y \langle H_u^0 \rangle & -\frac{1}{\sqrt{2}} g_2 \langle H_u^0 \rangle & -\mu & 0 \end{pmatrix},
 \end{aligned} \tag{5.18}$$

in the field basis

$$\begin{aligned}
 \tilde{\psi}^{+T} &= -i \left(\tilde{W}^+, i\tilde{H}_u^+ \right), \quad \tilde{\psi}^{-T} = -i \left(\tilde{W}^-, i\tilde{H}_d^- \right), \\
 \tilde{\psi}^{0T} &= -i \left(\tilde{B}, \tilde{W}^3, i\tilde{H}_d^0, i\tilde{H}_u^0 \right),
 \end{aligned} \tag{5.19}$$

for $\tilde{W}^\pm = (\tilde{W}^1 \mp i\tilde{W}^2)/\sqrt{2}$.

The one-loop beta function coefficients b_a and anomalous dimension γ_i in the MSSM are given by

$$\begin{aligned}
 b_3 &= -3, & b_2 &= 1, & b_1 &= \frac{33}{5}, \\
 \gamma_{H_u} &= \frac{3}{2} g_2^2 + \frac{1}{2} g_Y^2 - 3y_t^2,
 \end{aligned}$$

$$\begin{aligned}
 \gamma_{H_d} &= \frac{3}{2}g_2^2 + \frac{1}{2}g_Y^2 - 3y_b^2 - y_\tau^2 \\
 \gamma_{Q_a} &= \frac{8}{3}g_3^2 + \frac{3}{2}g_2^2 + \frac{1}{18}g_Y^2 - (y_t^2 + y_b^2)\delta_{3a}, \\
 \gamma_{U_a} &= \frac{8}{3}g_3^2 + \frac{8}{9}g_Y^2 - 2y_t^2\delta_{3a}, \\
 \gamma_{D_a} &= \frac{8}{3}g_3^2 + \frac{2}{9}g_Y^2 - 2y_b^2\delta_{3a}, \\
 \gamma_{L_a} &= \frac{3}{2}g_2^2 + \frac{1}{2}g_Y^2 - y_\tau^2\delta_{3a}, \\
 \gamma_{E_a} &= 2g_Y^2 - 2y_\tau^2\delta_{3a},
 \end{aligned} \tag{5.20}$$

where g_2 and $g_Y = \sqrt{3/5}g_1$ denote the $SU(2)_L$ and $U(1)_Y$ gauge couplings. The θ_i and $\dot{\gamma}_i$ which determine the soft scalar masses at M_{GUT} are given by

$$\begin{aligned}
 \theta_{H_u} &= 3g_2^2 + g_Y^2 - 6y_t^2(a_{H_u} + a_{Q_3} + a_{U_3}), \\
 \theta_{H_d} &= 3g_2^2 + g_Y^2 - 6y_b^2(a_{H_d} + a_{Q_3} + a_{D_3}) - 2y_\tau^2(a_{H_d} + a_{L_3} + a_{E_3}) \\
 \theta_{Q_a} &= \frac{16}{3}g_3^2 + 3g_2^2 + \frac{1}{9}g_Y^2 - 2\left(y_t^2(a_{H_u} + a_{Q_3} + a_{U_3}) + y_b^2(a_{H_d} + a_{Q_3} + a_{D_3})\right)\delta_{3a}, \\
 \theta_{U_a} &= \frac{16}{3}g_3^2 + \frac{16}{9}g_Y^2 - 4y_t^2(a_{H_u} + a_{Q_3} + a_{U_3})\delta_{3a}, \\
 \theta_{D_a} &= \frac{16}{3}g_3^2 + \frac{4}{9}g_Y^2 - 4y_b^2(a_{H_d} + a_{Q_3} + a_{D_3})\delta_{3a}, \\
 \theta_{L_a} &= 3g_2^2 + g_Y^2 - 2y_\tau^2(a_{H_d} + a_{L_3} + a_{E_3})\delta_{3a}, \\
 \theta_{E_a} &= 4g_Y^2 - 4y_\tau^2(a_{H_d} + a_{L_3} + a_{E_3})\delta_{3a},
 \end{aligned} \tag{5.21}$$

and

$$\begin{aligned}
 \dot{\gamma}_{H_u} &= \frac{3}{2}g_2^4 + \frac{11}{2}g_Y^4 - 3y_t^2b_{y_t}, \\
 \dot{\gamma}_{H_d} &= \frac{3}{2}g_2^4 + \frac{11}{2}g_Y^4 - 3y_b^2b_{y_b} - y_\tau^2b_{y_\tau}, \\
 \dot{\gamma}_{Q_a} &= -8g_3^4 + \frac{3}{2}g_2^4 + \frac{11}{18}g_Y^4 - (y_t^2b_{y_t} + y_b^2b_{y_b})\delta_{3a}, \\
 \dot{\gamma}_{U_a} &= -8g_3^4 + \frac{88}{9}g_Y^4 - 2y_t^2b_{y_t}\delta_{3a}, \\
 \dot{\gamma}_{D_a} &= -8g_3^4 + \frac{22}{9}g_Y^4 - 2y_b^2b_{y_b}\delta_{3a}, \\
 \dot{\gamma}_{L_a} &= \frac{3}{2}g_2^4 + \frac{11}{2}g_Y^4 - y_\tau^2b_{y_\tau}\delta_{3a}, \\
 \dot{\gamma}_{E_a} &= 22g_Y^4 - 2y_\tau^2b_{y_\tau}\delta_{3a},
 \end{aligned} \tag{5.22}$$

where

$$\begin{aligned}
 b_{y_t} &= -\frac{16}{3}g_3^2 - 3g_2^2 - \frac{13}{9}g_Y^2 + 6y_t^2 + y_b^2, \\
 b_{y_b} &= -\frac{16}{3}g_3^2 - 3g_2^2 - \frac{7}{9}g_Y^2 + y_t^2 + 6y_b^2 + y_\tau^2, \\
 b_{y_\tau} &= -3g_2^2 - 3g_Y^2 + 3y_b^2 + 4y_\tau^2.
 \end{aligned} \tag{5.23}$$

References

- [1] H. P. Nilles, Phys. Rept. **110**, 1 (1984); H. E. Haber and G. L. Kane, Phys. Rept. **117**, 75 (1985).
- [2] For a review, see G. Jungman, M. Kamionkowski and K. Griest, Phys. Rep. **267**, 195 (1996); G. Bertone, D. Hooper and J. Silk, Phys. Rep. **405**, 279 (2005) [arXiv:hep-ph/0404175]
- [3] D. N. Spergel *et al.* [arXiv:astro-ph/0603449].
- [4] S. B. Giddings, S. Kachru and J. Polchinski, Phys. Rev. **D66**, 106006 (2002) [arXiv:hep-th/0105097].
- [5] S. Kachru, R. Kallosh, A. Linde and S. P. Trivedi, Phys. Rev. D **68**, 046005 (2003) [arXiv:hep-th/0301240].
- [6] K. Choi, A. Falkowski, H. P. Nilles, M. Olechowski and S. Pokorski, JHEP **0411**, 076 (2004) [arXiv:hep-th/0411066]; K. Choi, A. Falkowski, H. P. Nilles and M. Olechowski, Nucl. Phys. **B718**, 113 (2005) [arXiv:hep-th/0503216].
- [7] V. S. Kaplunovsky and J. Louis, Phys. Lett. B **306**, 269 (1993) [arXiv: hep-th/9303040]; A. Brignole, L. E. Ibanez and C. Munoz, Nucl. Phys. B **422**, 125 (1994) [Erratum-ibid. B **436**, 747 (1995)] [arXiv: hep-ph/9308271].
- [8] L. Randall and R. Sundrum, Nucl. Phys. B **557**, 79 (1999) [arXiv: hep-th/9810155]; G. F. Giudice, M. A. Luty, H. Murayama and R. Rattazzi, JHEP **9812**, 027 (1998) [arXiv: hep-ph/9810442]; J. A. Bagger, T. Moroi and E. Poppitz, JHEP **0004**, 009 (2000) [arXiv: hep-th/9911029]; P. Binetruy, M. K. Gaillard and B. D. Nelson, Nucl. Phys. B **604**, 32 (2001) [arXiv: hep-ph/0011081].
- [9] K. Choi, K. S. Jeong and K. i. Okumura, JHEP **0509**, 039 (2005) [arXiv:hep-ph/0504037].
- [10] O. L.-Brito, J. Martin, H. P. Nilles and M. Ratz, hep-th/0509158
- [11] M. Endo, M. Yamaguchi and K. Yoshioka, Phys. Rev. **D 72**, 015004 (2005)[arXiv:hep-ph/0504036].
- [12] A. Falkowski, O. Lebedev and Y. Mambrini, JHEP **0511**, 034 (2005)[arXiv: hep-ph/0507110].
- [13] H. Baer, E.-K. Park, X. Tata and T. T. Wang hep-ph/0604253.
- [14] H. Baer, E.-K. Park, X. Tata and T. T. Wang, hep-ph/0607085.
- [15] M. Endo, K. Hamaguchi and F. Takahashi, Phys. Rev. Lett. **96** (2006) 211301 [arXiv:hep-ph/0602061]; S. Nakamura and M. Yamaguchi, Phys. Lett. B **638**, 389 (2006) [arXiv:hep-ph/0602081]; T. Asaka, S. Nakamura and M. Yamaguchi, Phys. Rev. **D74**, 023520 (2006) [arXiv:hep-ph/0604132]; M. Dine, R. Kitano, A. Morisse and Y. Shirman, Phys. Rev. **D73**, 123518 (2006) [arXiv:hep-ph/0604140]
- [16] J. Ellis, K. Olive and P. Sandick, hep-ph/0607002.
- [17] D. H. Lyth and E. D. Stewart, Phys.Rev. **D 53**, 1784 (1996) [arXiv:hep-ph/9510204]; Phys. Rev. Lett. **75**, 201 (1995) [arXiv:hep-ph/9502417]
- [18] T. Moroi and L. Randall, Nucl. Phys. B **570**, 455 (2000) [arXiv:hep-ph/9906527];
- [19] R. Dermisek and H. D. Kim, Phys. Rev. Lett. **96**, 211803 (2006) [arXiv:hep-ph/0601036]; R. Dermisek, H. D. Kim and I.-W. Kim, hep-ph/0607169.

- [20] J. A. Casas, A. Lleyda and C. Munoz, Nucl. Phys. **B471**, 3 (1996) [arXiv:hep-ph/9507294]
- [21] A. Kusenko, P. Langacker and G. Segre, Phys. Rev. **D54**, 5824 (1996) [arXiv:hep-ph/9602414]; A. Kusenko and P. Langacker, Phys. Lett. B **391**, 29 (1997) [arXiv:hep-ph/9608340].
- [22] A. Riotto and E. Roulet, Phys. Lett. B **377**, 60 (1996) [arXiv:hep-ph/9512401]
- [23] K. Choi and K. S. Jeong, arXiv:hep-th/0605108.
- [24] F. Brummer, A. Hebecker and M. Trapletti, hep-th/0605232.
- [25] K. Choi, Phys. Rev. Lett. **72**, 1592 (1994) [arXiv:hep-ph/9311352].
- [26] M. Luty and R. Sundrum, Phys. Rev. **D62**, 035008 (2000) [arXiv:hep-th/9910202]; Phys. Rev. **D64**, 065012 (2001) [arXiv:hep-th/0012158].
- [27] K. Choi and J. E. Kim, Phys. Lett. B **165**, 71 (1985); L. E. Ibanez and H. P. Nilles, Phys. Lett. B **169**, 354 (1986); T. Banks and M. Dine, Nucl. Phys. B **479**, 173 (1996) [arXiv:hep-th/9605136]; K. Choi, Phys. Rev. D **56**, 6588 (1997) [arXiv:hep-th/9706171].
- [28] D. Lust, P. Mayr, R. Richter and S. Stieberger, Nucl. Phys. **B696**, 205 (2004) [arXiv:hep-th/0404134].
- [29] H. Abe, T. Higaki and T. Kobayashi, D **73**, 046005 (2006) [arXiv:hep-th/0511160].
- [30] K. Choi, K. S. Jeong, T. Kobayashi and Ken-ichi Okumura, Phys. Lett. B **633**, 355 (2006) [arXiv:hep-ph/0508029]; R. Kitano and Y. Nomura, Phys. Lett. B **631**, 58 (2005) [arXiv:hep-ph/0509039]; O. Lebedev, H. P. Nilles and M. Ratz, arXiv:hep-ph/0511320; A. Pierce and J. Thaler, arXiv:hep-ph/0604192.
- [31] G. W. Bennett *et al.*, [Muon g-2 Collaboration], Phys. Rev. Lett. **92**, 161802 (2004) [arXiv:hep-ex/0401008]; M. Davier, S. Eidelman, A. Hocker and Z. Zhang, Eur. Phys. J. C **31** (2003) [arXiv:hep-ph/0308213]; K. Hagiwara, A. D. Martin, D. Nomura and T. Teubner, Phys. Rev. D **69**, 093003 (2004) [arXiv:hep-ph/0312250]; J. F. de Troconiz and F. J. Yndurain, arXiv:hep-ph/0402285; K. Melnikov and A. Vainshtein, arXiv:hep-ph/0312226; M. Passera, arXiv:hep-ph/0411168.
- [32] P. Gondolo, J. Edsjo, L. Bergstrom, P. Ullio and E. A. Baltz, arXiv:astro-ph/0012234; P. Gondolo, J. Edsjo, P. Ullio, L. Bergstrom, M. Schelke and E. A. Baltz, JCAP 0407 (2004) 008 [arXiv:astro-ph/0406204].
- [33] M. W. Goodman and E. Witten, Phys. Rev. **D 31** (1985) 3059.
- [34] SuperCDMS, arXiv:astro-ph/0503583.
- [35] J. Diemand, B. Moore and J. Stadel, Mon. Not. Roy. Astron. Soc. **353**, 624 (2004); B. Moore *et al.*, Astrophys. J. **524**, L19 (1999).
- [36] F. Aharonian *et al.*, The HESS collaboration, astro-ph/0408145.
- [37] G. Zaharijas and D. Hooper, Phys. Rev. **D 73**, 103501 (2006).
- [38] S. Mizuta and M. Yamaguchi, Phys. Lett. B **298** (1993) 120 [arXiv:hep-ph/9208251]; U. Chattopadhyay, D. Choudhury, M. Drees, P. Konar and D. Roy, Phys. Lett. B **632** (2006) 114 [arXiv:hep-ph/0508098].
- [39] L. Bergstrom, P. Ullio and J.H. Buckley, Astropart Phys. **9**, 137 (1998); P. Ullio and L. Bergstrom, Phys. Rev. D **57**, 1962 (1998).